DESIGN AND MODEL OF NITRIC OXIDE DELIVERY TO CELLS

By

SHRAVAN NAGARAJAN

Bachelor of Engineering

University of Poona

Pune, India

1994

Submitted to the Faculty of the
Graduate College of the
Oklahoma State University
in partial fulfillment of
the requirements for
the degree of
MASTER OF SCIENCE
May, 1997

DESIGN AND MODEL OF NITRIC OXIDE DELIVERY

TO CELLS

Thesis Approved:

Randy S. Lewis
Thesis Adviser

Arlund H. Johannes

Gary L. Foutch

Thomas C. Collins
Dean of the Graduate College

ACKNOWLEDGMENT

First and foremost, I thank the Almighty for bringing me to this stage in my life and for having seen me safely through good times and bad. Respectful thanks are due to my parents, Vijaya and R. Nagarajan for their love and support , and for always being there when I have needed help, consolation, or guidance. Special thanks are also due to the numerous people in Tulsa who came to my aid in my time of need. Among them, I would especially like to thank Mr. Umanath, Mr. Swaminathan, Mr. M.T. Srinivasan, and Dr. Jayaram, their spouses, and families. I reserve special thanks for Dr. Kache for being instrumental in my recovery to good health after my accident. I express immense gratitude to Dr. Randy Lewis for providing understanding and inspirational guidance throughout my period of graduate study in addition to providing financial and moral support. I consider myself fortunate to have worked under him.

I thank Dr. Johannes and Dr. Foutch for serving on my thesis committee. I am grateful to Dr. McCann for allowing me access to his research facilities and Denise for having helped me in my work there. I also thank Charles Baker, the staff of Chemical Engineering, and Mike Lucas for their assistance. I thank Joseph, Anand, Mahendra, Satyanarayan, Baskar, Bhagyalakshmi, and all my numerous friends in Stillwater for their help and companionship.

TABLE OF CONTENTS

LIST OF TABLES

LIST OF FIGURES

CHAPTER 1

INTRODUCTION

Nitric oxide (NO) is a highly reactive free radical gas that is colorless and odorless at room temperature. It is known to be a toxic atmospheric pollutant that also causes ozone layer depletion [Coolman and Robarge, 1995]. NO was identified as a biological molecule upon demonstration, in 1987, of its generation by an enzyme [Moncada et al., 1989]. This has lead to an increase in research activity investigating nitric oxide's physiological functions and pathological effects.

NO is synthesized endogenously by many mammalian cells including macrophages, neutrophils, endothelial cells, and hepatocytes [Conner and Grisham, 1993]. Endogenous NO is also present in the exhaled air from animals and humans in concentrations on the order of 10 ppb [Gustafsson et al., 1991]. NO has several important physiological roles such as blood pressure regulation, neurotransmission, and immunoregulation. However, the underproduction or overproduction of NO is at least partly responsible for the pathogenesis of several conditions such as hypertension, septic shock, and perhaps cirrhosis and diabetes [Moncada and Higgs, 1993; Corbett et al., 1993].

1.1 Biosynthesis of nitric oxide.

NO is produced in vertebrate cells by the enzyme catalyzed oxidation of L-arginine to citrulline. This enzyme, called nitric oxide synthase (NOS), may be present in cells as a constitutive and/or inducible enzyme. The constitutive isoform of NOS (cNOS) is Ca^{2+} /

calmodulin dependent and is activated by stimuli such as pulsatile blood flow or shear stress due to increased blood flow. Activation of this enzyme causes a short-lasting release of NO on the order of a few picomoles mg^{-1} min^{-1} [Conner and Grisham, 1993]. This release is inhibited by L-arginine analogs but not glucocorticoids. The inducible isoform of NOS (iNOS), on the other hand, is controlled at the transcriptional level and is activated by cytokines and bacterial endotoxins. It is Ca^{2+} / calmodulin independent and causes a long-lasting release of NO on the order of nanomoles mg^{-1} min^{-1} [Conner and Grisham, 1993]. The induction of iNOS is inhibited by glucocorticoids and its function is inhibited by L-arginine analogs. The inducible form of NOS is mainly found in macrophages and, in some cases, other cells such as endothelial cells and pancreatic β-cells [Kroncke et al., 1995].

1.2 NO in the cardiovascular and pulmonary system.

In the cardiovascular system, NO is essential for regulating blood flow and blood pressure [Moncada, 1992]. NO in synergy with prostacyclin inhibits platelet aggregation which prevents clots from forming in the blood vessels. NO acting alone inhibits platelet adhesion [Radomski and Moncada, 1991] as well as adhesion of leucocytes to the microvascular endothelium [Kubes et al., 1991] and the resultant endothelial injury. In the pulmonary system, inhaled NO has been found to reverse pulmonary hypertension [Pepko-Zaba et al., 1991] and protect against respiratory distress syndrome [Rossaint et al., 1993]. The calcium independent isoform of NOS can be induced in smooth muscle cells as well as in endothelial cells. The generated NO leads to vascular relaxation that cannot be reversed by vasoconstrictors. This vasodilation and resistance to vasoconstrictors is

characteristic of septic shock as well as hypotension induced by cytokine therapy in patients with cancer [Moncada, 1992]. Generation of large quantities of NO by iNOS may lead to tissue damage, cirrhosis [Vallance and Moncada, 1991] and cardiac dysfunction associated with dilated cardiomyopathy (primary myocardial disease) [de Belder et al., 1993]. The underproduction of NO leads to hypertension.

1.3 NO in the gastrointestinal system.

In addition to maintaining vasodilator tone in the gastrointestinal system, NO in synergy with prostacyclin apparently maintains the integrity of the mucosal layer. NO also appears to mediate some forms of muscular relaxation including the dilation of the stomach to adapt to increases in intragastric pressure [Rand, 1992], the relaxation of the circular sigmoid muscle of the colon [Tam and Hiller, 1992], and the anal spincter muscle [Burleigh, 1992]. NO may be the key to finding a cure for impotence as it is responsible for effecting penile erection [Ignarro et al., 1990].

As in the cardiovascular system, NO-dependent dilator tone is essential for proper functioning of the organs. Inadequate production of NO in the corpus cavernosum (spongy body of the penis) may be the cause for male impotence while deficiency of NOS in the pyloric tissue is the cause of hypertropic pyloric stenosis (blockage of the passage connecting the stomach to the duodenum) in infants [Vanderwinden et al., 1992]. A deficiency of NOS in adult gastrophageal tissue seems to be the cause of achalasia (failure of smooth muscle in the gastrointestinal tract to relax) [Mearin et al., 1993].

1.4 NO in the central nervous system.

In the brain, NO is responsible for a phenomenon known as long-term potentiation that is thought to be linked to memory formation [Collingridge et al., 1983]. NO may also have a physiological role in vision, feeding behavior, and olfaction [Moncada and Higgs, 1993].

NO cytotoxicity resulting from its overproduction may be partially responsible for stroke, Huntingdon's chorea, cerebral ischemia (deficiency of blood in the brain), epilepsy [Moncada et al., 1989], multiple sclerosis, Alzheimer's disease, Parkinson's disease, and dementia of acquired immune deficiency syndrome [Moncada and Higgs, 1993].

1.5 NO as a cytotoxic and cytostatic agent.

Macrophages and neutrophils synthesize NO as a defense against microorganisms such as bacteria [Hibbs et al., 1990]. The biochemical basis for this cytotoxicity of NO is the reaction of NO with iron containing moieties in key enzymes of the respiratory cycle and/or DNA damage in the target cells [Moncada and Higgs, 1993]. NO is thus involved in non-specific immunity and the seemingly non-specific nature of its cytotoxicity may prove to be deleterious not only for tumor cells and invading microorganisms but also for NO generating cells and their immediate neighbors. The NO generated by iNOS could thus be responsible for the damage of healthy and normal tissue leading to the pathogenesis of rheumatoid arthritis, ulcerative colitis [Moncada and Higgs, 1993], insulin dependent diabetes mellitus (IDDM) [Bendtzen, 1989] and asthma [Moncada, 1994]. Inhibition of NO generation by introducing L-arginine analogs is shown to alleviate inflammation and adjuvant arthritis in rats [Moncada and Higgs, 1993].

1.6 Biological reactions of nitric oxide.

The biological actions of NO differ from other major mediators in that (a) its functions are governed by its chemical properties as opposed to its shape, (b) it can diffuse freely from the site of synthesis to the adjacent tissues, and (c) no enzymatic mechanism is required for its removal [Conner and Grisham, 1995]. As a very reactive molecule, NO reacts with several species in aqueous media. The byproducts of some of these reactions may also be of physiological and pathological significance.

1.6.1 Reaction with oxygen.

NO reacts with the dissolved oxygen in the following manner.

$$2\,NO + O_2 \longrightarrow 2\,NO_2 \qquad (1.1)$$

$$NO + NO_2 \longrightarrow N_2O_3 \qquad (1.2)$$

Nitrous anhydride (N_2O_3) then decomposes in aqueous media to form nitrite (NO_2^-) [Lewis and Deen, 1994] according to

$$N_2O_3 + H_2O \longrightarrow 2\,H^+ + 2\,NO_2^- \qquad (1.3)$$

Nitrous anhydride is a nitrosating agent and thus a cytotoxin that denatures DNA by nitrosation of the primary amines on DNA bases. It also may nitrosate secondary amines to yield carcinogenic and mutagenic products [Tannenbaum et al., 1991]

1.6.2 Reaction with superoxide.

Superoxide (O_2^-) is an oxygen free radical that is co-synthesized with NO by

macrophages and neutrophils during immunological reactions. It reacts with NO to form the peroxinitrite ($ONOO^-$) radical [Huie and Padmaja, 1993].

$$NO^{\cdot} + O_2^{\cdot-} \longrightarrow ONOO^- \qquad (1.4)$$

Peroxinitrite is a strong oxidant that reacts in aqueous medium to form a very highly reactive "hydroxyl-like" radical [Beckman et al., 1990b]. Peroxinitrite and the hydroxyl ion can cause lipid membrane peroxidation [Hogg et al., 1992] and the denaturing of DNA [Delaney and Eizirik, 1996].

1.6.3 Reaction with the sulphydryl groups.

NO reacts with the sulphydryl groups on proteins to form S-nitrosothiols which are more stable than NO. Therefore, the sulphydryl groups on proteins are potential NO carriers. S-nitrosothiols are potent vasodilators and platelet inhibitors [Stamler et al., 1992].

1.6.4 Reaction with metalloproteins.

The interactions of NO with metalloproteins constitute relevant molecular mechanisms accounting for its signal transduction and cytotoxicity. NO readily reacts with the metal centers of proteins including iron, iron-sulfur and zinc-sulfur clusters [Radi, 1996]. These interactions with NO lead to the formation of a metal nitrosyl complex resulting in a modification of the structure and/or function of these proteins.

In blood, excess NO is scavenged by oxyhemoglobin to form met-hemoglobin and nitrate, or deoxyhemoglobin to form a stable iron nitrosyl complex with its iron core. This depletes NO produced in tissues and characterizes NO as a local signal transduction

molecule [Radi, 1996]. NO also reacts with the iron core in cytochrome c oxidase and cytochrome P450 which leads to inhibition of mitochondrial electron transport [Cleeter et al., 1994].

The interaction of NO with the iron-sulfur cluster of mitochondrial aconitase results in the inhibition of Krebs cycle resulting from enzyme inactivation [Radi, 1996]. The interaction of NO with zinc present in the zinc-sulfur cluster of enzyme alcohol dehydrogenase leads to inhibition of the DNA binding ability of the enzyme [Radi, 1996].

1.7 NO and Diabetes Mellitus.

Clinical diabetes mellitus is a syndrome of inadequate glucose metabolism causing inappropriately high levels of glucose in the blood. This may occur due to a total absence of the hormone insulin or a reduction in the biological effectiveness of insulin. Diabetes is classified as insulin dependent (type 1) or non-insulin dependent (type 2). Type 1 is a severe ailment characterized by an almost total absence of insulin due to death or severe dysfunction of the β cells in pancreatic islets. It is an autoimmune disease in which NO is believed to be one of the mediators of cell death [McDaniel et al., 1996]. This thesis develops and models the system in which β cells could be exposed to controlled concentrations of NO to quantify the effect of NO on cell viability and insulin secretion.

CHAPTER 2

NITRIC OXIDE: A MEDIATOR OF PANCREATIC β-CELL DYSFUNCTION?

Insulin-dependent diabetes mellitus is an autoimmune disease which appears to develop over a long period of time before becoming clinically manifest [Eisenbarth, 1986]. This prediabetic period is characterized by inflammatory reaction in the vicinity of the pancreatic islets and infiltration of the islets by macrophages and lymphocytes resulting specifically in the death of the insulin producing β-cells [Mandrup-Poulson et al., 1990; Castano and Eisenbarth, 1990]. Inflammatory products of these macrophages such as cytokines and free radicals have been implicated in the destruction of pancreatic β-cells [Corbett and McDaniel, 1992]. Cytokines are glycoproteins synthesized in a variety of different cells, in response to numerous stimuli, that act in picomolar to nanomolar quantities to regulate target cell function [Nathan and Sporn, 1991].

Two models have been proposed in which NO appears to be responsible for β-cell death. The first is that the release of cytokines by activated macrophages in the vicinity of the β-cells induces endogenous NO production in the β-cells, resulting in self destruction [Corbett and McDaniel, 1992]. The second model is a scenario in which cytokine activated macrophages and pancreatic endothelial cells produce large amounts of NO which, acting alone or in cooperation with oxygen free radicals, lead to β-cell destruction [Kolb and Kolb-Bachofen, 1992]. Much of the research investigating NO cytotoxicity has focused on determining the effects of cytokines [Dunger et al., 1996; Rabinovitch et al., 1990], cytokine induced NO [Corbett et al., 1993; Dunger et al., 1996], and intracellularly

and extracellularly generated NO, using NO-donor compounds [Eizirik et al., 1996], on the function and viability of pancreatic β-cells.

2.1 Effects of intracellular NO generation.

Macrophage generated cytokines, primarily interlukin-1β (IL-1β), tumor necrosis factor α (TNF-α), and interferon γ (INF-γ) induce NO formation in β-cells [Corbett and McDaniel, 1992]. The endogenously generated NO can inhibit the normal endocrine function of the β-cells by obstructing their mitochondrial function [Drapier et al., 1986] or by causing cell death by initiating DNA strand breaks [Fehsel et al., 1993; Delaney and Eizirik, 1996]. Similar effects have been observed when using compounds that generate NO intracellularly [Green et al., 1993].

2.1.1 Effects of cytokine induced NO.

The results of the experiments aimed at determining the effect of cytokines and cytokine induced NO on β-cells have been varied and often contradictory [Corbett et al., 1993; Eizirik et al., 1994, Suarez-Pinzon et al., 1994; Corbett and McDaniel, 1995]. This is likely due to 1) use of cells extracted from different mammalian species such as rats, mice and humans [Kawahara and Kenney, 1991]; 2) different methods of cell preparation (islet culture vs culture of purified β-cells as a monolayer) since the matrix can control how cells respond to cytokines [Nathan and Sporn, 1991]; 3) the species the cytokines were obtained from [Pukel et al., 1988]; 4) the concentrations of cytokines and exposure times.

2.1.1.1 Effect of NO on rat pancreatic islets.

Rat pancreatic islets are by far the most susceptible to the effects of cytokines and cytokine induced NO [Welsh et al., 1994] when compared with islets from mice and humans. Several researchers [Corbett et al., 1992; Corbett and McDaniel, 1995; Dunger et al., 1996] have observed IL-1β induced NO generation in rat β-cells paralleled by significant inhibition of glucose oxidation, inhibition of glucose stimulated insulin secretion, and DNA damage. However, other researchers have been able to dissociate the inhibitive actions of IL-1β from those of IL-1β induced NO and claim that IL-1β induced inhibition of β-cell function and the subsequent cell death follow NO-dependent as well as NO-independent pathways [Anderson et al., 1994; Suarez-Pinzon et al., 1994]. In a monolayer culture of rat β-cells, lysis was observed only when the cells were exposed to combinations of IL-1, TNF-α and INF-γ obtained from rodents. Individually, these cytokines, as well as human cytokines, did not exhibit any cytotoxicity towards rat β-cells [Pukel et al., 1988].

2.1.1.2 Effect of NO on murine pancreatic islets.

In murine islets, the presence of TNF-α or INF-γ in addition to IL-1 was necessary to induce NO production [Rabinovitch et al., 1996]. Cytokine induced NO was at least partially responsible for inhibition of insulin secretion [Welsh and Sandler, 1992] by murine islets. However, the inhibition of insulin secretion was achieved without impairing β-cell mitochondrial function.

2.1.1.3 Effect of NO on human pancreatic islets.

Human pancreatic islets seem to be the least susceptible to the cytotoxic effects of cytokines [Eizirik et al., 1993]. Cytokines IL-1β, TNF-α, and INF-γ, were found to cause human β-cell lysis when a monolayer of β-cells was exposed to the individual cytokines. The β-cells were more potently lysed when exposed to a combination of all three cytokines [Rabinovitch et al., 1990]. However, insulin secretion was slightly stimulated by exposure to a combination of IL-1β, TNF-α, and INF-γ [Corbett et al., 1993]. NO generation in human islets was found to take place only in the presence of more than one cytokine, as in murine islets [Rabinovitch et al., 1994]. In some cases, [Corbett et al., 1993] cytokine induced NO was partially responsible a for decrease in islet function, while in other cases [Rabinovitch et al., 1994; Eizirik et al., 1994] islet function was totally unimpaired by cytokine induced NO.

2.1.2 Effects of intracellularly generated NO.

Chemicals such as hydroxylamine and Roussin's black salt (RBS) cause intracellular NO release. Hydroxylamine has been proposed to be an intermediate in the arginine-NO pathway [DeMaster et al., 1989]. The oxidation of hydroxylamine to NO is catalyzed by oxidative enzymes such as catalase that are present in all cells. RBS, on the other hand, contains iron-sulfur cluster nitrosyls containing 7.0 moles of ligated NO per mole of RBS. RBS is lipid soluble and accumulates in cell membranes acting as a protracted source of NO [Eizirik et al., 1996]. However, RBS also decomposes in solution releasing NO, iron, and sulfur.

Hydroxylamine has been used with rat [Green et al., 1993] and mouse [Panagiotidis et al., 1995] islets. In these rodent islets, hydroxylamine greatly inhibited islet insulin secretion. RBS also causes inhibition of insulin release in human and rat pancreatic islets. However, the effect is more potent in rat islets [Eizirik et al., 1996].

2.2 Effect of extracellularly generated NO.

NO-donor compounds such as sodium nitroprusside (NP) [Kroncke et al., 1993; Eizirik et al., 1994], 3-morpholinosydnonimine (SIN-1) [Green et al., 1993; Eizirik et al., 1996; Panagiotidis et al., 1995; Delaney et al., 1993; Kroncke et al., 1993], S-nitroso-N-acetyl-penicillamine (SNAP) [Kroncke et al., 1993; Green et al., 1993], S-nitrosoglutathione (GSNO) [Green et al., 1993; Eizirik et al., 1996], and streptozotocin (STZ) [Eizirik et al., 1994; Kaneto et al., 1995; Zuccollo et al., 1995] have been used to study the effects of NO on β-cells. All of these compounds release NO spontaneously in solution, except SNAP and GSNO whose decomposition is catalyzed by external vascular membranes [Kowaluk and Fung, 1990].

Researchers using NO-donor compounds have reported NO-dependent inhibition of insulin secretion accompanied by cell lysis in β-cells obtained from rats [Green et al., 1993; Eizirik et al., 1994; Delaney et al., 1993; Kroncke et al., 1993], mice [Eizirik et al., 1994; Zuccollo et al., 1995; Panagiotidis et al., 1995] and humans [Eizirik et al., 1994; Eizirik et al., 1996]. The experiments, however, seem to be plagued with several problems that introduce uncertainty in the interpretation of the results.

2.2.1 Shortcomings in experiments with NO-donor compounds.

The experiments using NO-donor compounds to evaluate the effect of NO on pancreatic β-cells have the following drawbacks:

1) Several of the compounds release additional species such as superoxide, as in the case of SIN-1 [Green et al., 1993]. Superoxide reacts with NO to form peroxinitrite, a species more damaging than NO [Huie and Padmaja, 1993]. Another compound, STZ, is an alkylating agent in addition to releasing NO [Kaneto et al., 1995] and may cause damage through NO independent-pathways. A study using STZ as a NO-donor compound showed that NO concentrations relatively lower than those produced by IL-1β in rat islets led to cell lysis [Kaneto et al., 1995]. This may indicate the existence of NO-independent cytotoxic mechanisms.

2) NO-donor compounds do not release NO at a steady rate. Thus, the NO concentration vs time profile is not necessarily constant [Ramamurthi, 1996]. This implies that NO concentrations may reach very high and physiologically unrealistic values. In addition, the cells are exposed to an unsteady-state NO concentration profile. In most experiments, a known amount of NO-donor compound is used without any reference to the kinetics of NO release by that compound.

3) The experiments are conducted in unstirred containers having a small volume of stagnant culture medium. There is no assurance that all the cells see the same concentrations of NO. There is also an accumulation of NO and its reaction products with other species in the aqueous medium that may prove to be detrimental to the function of the cells.

4) Chemical donor-generated NO is β-cell non-specific [Kroncke et al., 1993], causing damage to all the islet cells. However, pancreases from animals and humans with IDDM are deficient in β-cells alone [Foulis, 1987]. This may be the result of the above mentioned defects in the experiments using chemical NO donors.

2.3 Thesis Objectives.

The thesis objective is to design a system to achieve controlled and steady-state NO concentrations in the aqueous phase to which the cells are exposed (explained in Chapter 3). This would eliminate the use of NO-donor compounds and the accompanying experimental uncertainties. The specific aims of the thesis are defined below.

2.3.1 Specific Aim #1.

The first aim is to design and build an apparatus capable of delivering NO in the aqueous phase to pancreatic β-cells. The delivery should be designed for a wide range of steady-state NO concentrations in an environment that provides no other species for NO to react with, except the dissolved oxygen, while ensuring that all the cells present in the apparatus are exposed to the same NO concentration. The system should also be designed so that there is no accumulation of NO or its reaction products in the vicinity of the cells.

2.3.2 Specific Aim #2.

The second aim is to model the NO delivery device and the subsequent reaction with the dissolved oxygen to predict the NO concentration to which the cells will be exposed. This will be achieved by adapting an existing model (explained in Chapter 4) to predict the aqueous NO concentration at the delivery device outlet. Equations that describe the

downstream liquid mixing behavior and those that quantify the reaction of NO with dissolved oxygen will be used to predict the NO concentration in the vicinity of the cells. The model will be validated at room temperature and physiological temperature (37°C) by measuring the NO concentration with a NO probe.

2.3.3 Specific Aim #3.

The final aim of this thesis is to perform experiments involving the exposure of β-cells to controlled NO concentrations and establish the procedure for performing the experiments and the subsequent sample assays. A few experiments will be performed to ascertain whether the system can be used to study the effects of NO on β-cells. Samples will be collected and assayed to determine insulin content and to ascertain whether extracellularly-generated NO affects β-cell function.

CHAPTER 3

AQUEOUS NITRIC OXIDE DELIVERY: DESIGN CONSIDERATIONS

The study of the effect of NO on living systems requires an effective method for NO delivery in the aqueous phase. Aqueous NO delivery can be achieved either chemically with NO-donor compounds or physically by the mass transfer of gaseous NO to the liquid phase.

3.1 Chemical method of NO delivery.

Certain compounds such as SIN-1 and NONOates release NO in solution. Some of these compounds have potential medical use in treating hypertension, penile erectile dysfunction, respiratory distress syndrome, and some heart ailments [Kerwin et al., 1995]. The NO-release kinetics of spermine and diethylamine NONOates have been characterized and modeled [Ramamurthi, 1996]. The release rate varies with time resulting in an unsteady-state concentration vs time profile in many experimental systems.

3.2 Physical method of NO delivery.

The physical method of NO delivery uses a semi-permeable membrane to separate a flowing stream of liquid from a gas phase containing NO while allowing mass transfer of NO across the membrane. The gas phase consists of a mixture of NO with an inert gas such as nitrogen. The desired aqueous NO concentration is achieved by controlling the partial pressure of NO in the gas phase, the liquid flowrate, and the area available for mass transfer.

3.3 Design of NO delivery device.

The delivery of NO is achieved by mass transfer of gaseous NO to pH 7.4 aqueous phosphate buffer across a flat sheet of polydimethylsiloxane (Silastic®) membrane. A previous method to deliver NO to the aqueous phase used Silastic® tubing [Tamir et al., 1993]. However, the concentration was not predictable using this method. The present design uses a Silastic® sheet in preference to Silastic® tubing as the NO delivery rate vs partial pressure ([NO] vs P_{NO}) data obtained using the Silastic® sheet were found to be linear in contrast to the non-linearity with the tubing.

The NO delivery device permits liquid flow through a conduit of rectangular cross-section bounded at the top and bottom by sheets of Silastic®. NO gas flowing on the outside of the Silastic® membranes initiates diffusion through the membranes and into the liquid. The benefits of choosing a configuration where NO diffuses across semi-permeable membranes enclosing a flowing stream of liquid are 1) the ability to control the rate of NO transport into solution, and 2) knowledge of the steady-state solution to equations predicting the mass transfer rate of a species from gas to liquid across membranes enclosing the liquid stream.

3.3.1 Physical characteristics and sizing.

The delivery device consists of three longitudinal parts made of stainless steel and held together by stainless steel Allen-head screws (see Figure 3.1). The central part has an inlet and an outlet for liquid at both ends of a 15.3 cm long rectangular slot having a cross-section 0.5 cm wide × 0.3 cm deep. The ends of the slot were rounded to minimize entrance and exit effects. The slot was bounded at the top and bottom by two sheets of

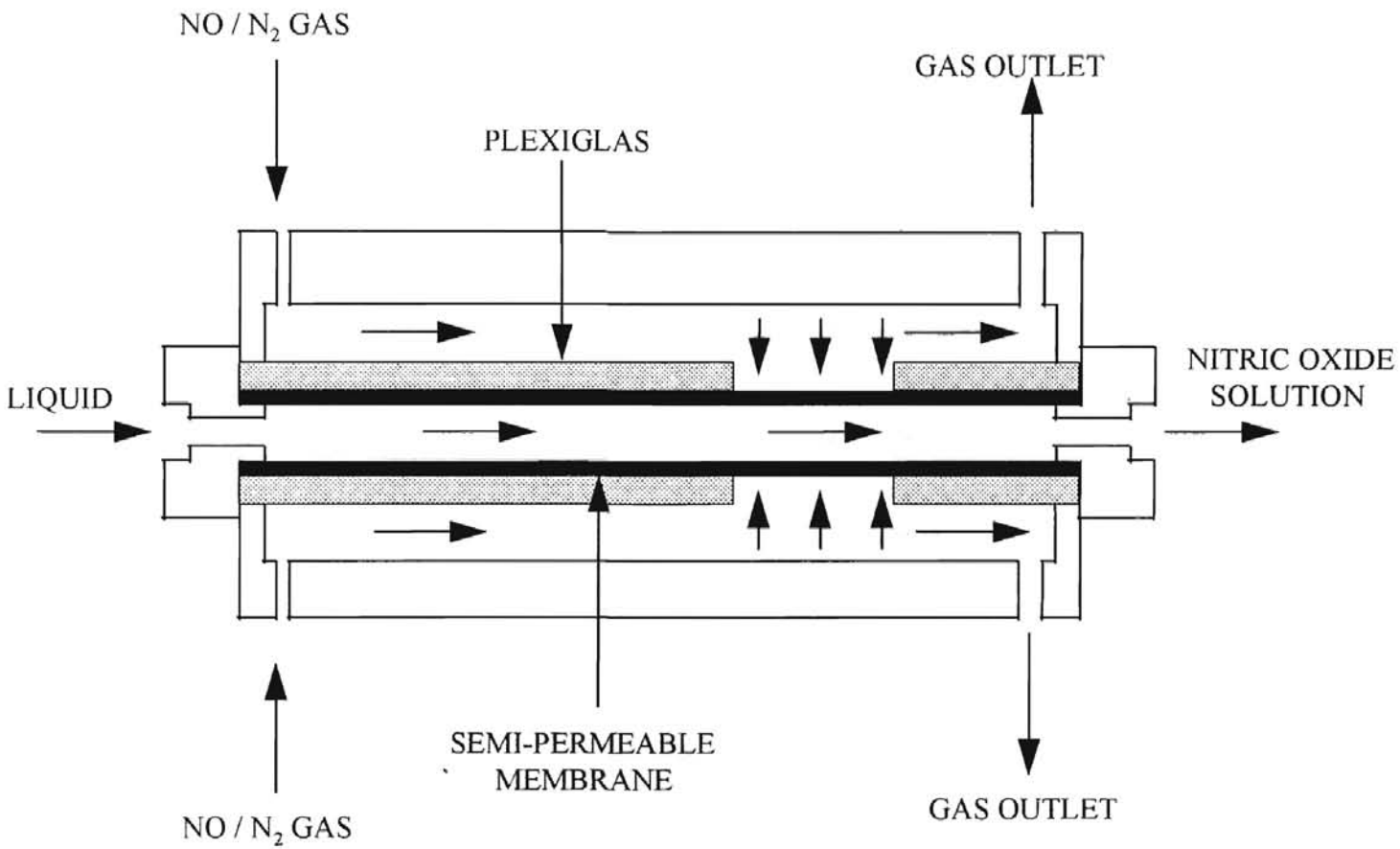

Figure 3.1. Nitric oxide delivery device (See text for dimensions).

5 mil Silastic® membrane laminated to 0.16 cm thick rectangular sheets of plexiglas using silicone adhesive. The membranes which are compressed between the plexiglas and steel prevent liquid leaks while also preventing the entry of air into the liquid stream. Each plexiglas sheet contains a 2.5 cm long×0.5 cm wide rectangular opening that is 10.2 cm from the liquid inlet. The opening was thus placed in order to minimize the reaction of NO with dissolved oxygen inside the delivery device while ensuring that the flow is fully developed before it reaches the opening. The liquid flow is maintained at 3.0 ml/min using a peristaltic pump.

The plexiglas opening exposes the membrane to the gas by providing a permeable interface for mass transfer into the liquid. The NO delivery rate is controlled by varying the length of the opening and hence the mass transfer area. Maximum delivery can be achieved by increasing the plexiglas opening length to 15.3 cm which is the length of the slot containing the liquid. In addition, chambers 15.3 cm long, 0.5 cm wide, and 0.3 cm deep were fabricated above and below the central portion of the device. The chambers were designed to allow gas to enter via an inlet, partially diffuse across the membrane into the liquid through the openings in the plexiglas, and leave through an outlet. Gas leaks from the chambers are prevented by two rubber gaskets placed in between the plexiglas sheets and chambers.

3.4 Design of the vessel containing the cells.

A vessel for containing the cells was designed to be placed downstream of the delivery device. This vessel was designed to hold a sufficient number of cells to produce

detectable insulin concentrations while ensuring exposure of all the cells to a uniform and steady-state NO concentration as stated in Aim #1.

3.4.1 Design requirements.

In order to satisfy Aim #1, the vessel for containing the cells must have the following characteristics:

1) The vessel must have a large area to contain a sufficient number of β-cells, grown as a monolayer, to produce a detectable concentration of insulin in the liquid.

2) The NO concentration in the vessel must be uniform.

3) The volume of the vessel should be as small as permissible (by requirement #1), so that the formation of any reaction products of NO with the components of the buffer/culture medium would be minimized. This would reduce or eliminate the uncertainty following experiments that any observed effects on cells are caused by species other than NO.

3.4.2 Physical characteristics.

Based on the criteria outlined in the preceding section, a stirred vessel that would approximate an ideal continuous stirred tank reactor (CSTR) was desired to hold the cells. The following design decisions were made.

1) The vessel was to be constructed of stainless steel to protect it from corrosion by NO and to eliminate the formation of additional species by reaction with the vessel that would introduce uncertainty in the results. A stainless steel construction would be autoclavable.

2) The stirring would be achieved using a magnetic stirrer to rotate a stirbar made of magnetic material that would not react with NO or be oxidized by the culture medium.

3) The clearance between the stirbar and the bottom of the vessel would be sufficient to minimize the shear on the cells caused by the stirring.

4) For future work, an additional chamber to contain macrophages, separated from the stirred chamber by a semi-permeable membrane, would be provided.

5) The liquid inlet would be at the base of the vessel while the outlet would be near the top. This would facilitate removal of air bubbles when filling the vessel.

3.4.3 Vessel sizing and operating conditions.

The diameter of the vessel was determined by calculating the area required to contain a monolayer of β-cells that would generate detectable amounts of insulin. This was accomplished using the basal (unstimulated or minimally stimulated by glucose) rate of insulin secretion of several cell types as reported in literature. A liquid flowrate of 3.0 ml/min was chosen based on economic considerations. A liter of culture medium costs ~$15. Therefore for a ten hour long experiment using nearly 2 liters, the cost would be $30. A low flowrate would also ensure laminar flow which is essential for modeling the mass transfer.

The minimum number of cells necessary to achieve a detectable insulin concentration and the area required to contain the cells were estimated for Rat β-cells [Corbett and McDaniel, 1995], Syrian hamster β-cells [Santerre et al., 1981], and the tumor cell lines INS-1 [Asfari et al., 1992] and HIT-5B5 [Santerre et al., 1981] using their basal insulin secretion rates. The results are summarized in Table I.

TABLE 1

INSULIN SECRETION BY VARIOUS CELL TYPES AND VESSEL SIZING

Cell Type	Rat	Hamster	INS-1	HIT-5B5
Basal Insulin Secretion ($\mu U/min/10^6$ cells)	79.8	270.0	191.4	20.0
Basal Insulin Concentration at CSTR outlet ($\mu U/ml/10^6$ cells)	26.6	90.0	63.8	6.67
Minimum Number of Cells	6×10^4	2×10^4	2.5×10^4	2.3×10^6
Minimum Vessel Diameter (cm)	0.42	0.32	0.27	1.07
Stimulated Insulin Concentration at CSTR outlet ($\mu U/ml$, based on the minimum number of cells)	13.6	12.2	3.5	3.07
Glucose Concentration for stimulation (mM)	20	10	20	10

Note: The diameter of rat β-cells and INS cells is ~15 μm while that of hamster β-cells and HIT cells is ~20 μm.

A sample calculation using rat β-cells follows. The basal rate of insulin secretion by rat β-cells is 1 ng/2000 cells/3 hours which is equivalent to 2.78 ng/min/10^6 cells. Using the molecular weight for human insulin, which is 5808 Da, and the fact that 6.0 nmoles of insulin equal one International Unit [Volund, 1993] (the unit for measurement of proteins such as enzymes, cytokines, hormones etc., represented as U) the rate is 79.77 μU/min/10^6 cells. Therefore, the insulin concentration at the CSTR outlet is 26.6 μU/ml/10^6 cells for a flowrate of 3.0 ml/min. For a radioimmunoassay (RIA) sensitivity of 1.5 μU/ml (CoatACount, Diagnostic Products Corporation, Los Angeles, CA) this corresponds to a minimum number of cells of approximately 60,000. Assuming an average cell diameter of 15 μm [Bonner-Weir, 1991], the minimum area required for these cells, each of which is assumed to occupy a square whose side is equal to the cell diameter, is 0.135 cm^2. A stirred vessel of 0.42 cm diameter would have this area.

Since rat β-cells required the largest vessel diameter, except for HIT cells, and provided a comparatively higher concentration of insulin in the liquid outlet stream, the vessel sizing was based on data for these cells. The minimum number of rat β-cells required (see Table I) was multiplied by a factor of 10 to provide a margin of safety for the vessel diameter design. This cell number was again multiplied by 10 to account for the possibility of reduced insulin release by dysfunction or death of cells following exposure to NO. Therefore, a vessel diameter of 5.4 cm is required to contain 6.0×10^6 cells.

A vessel of 5.5 cm diameter (see Figure 3.2) was fabricated from stainless steel (SS304). It should be noted that the actual number of cells used may be less than

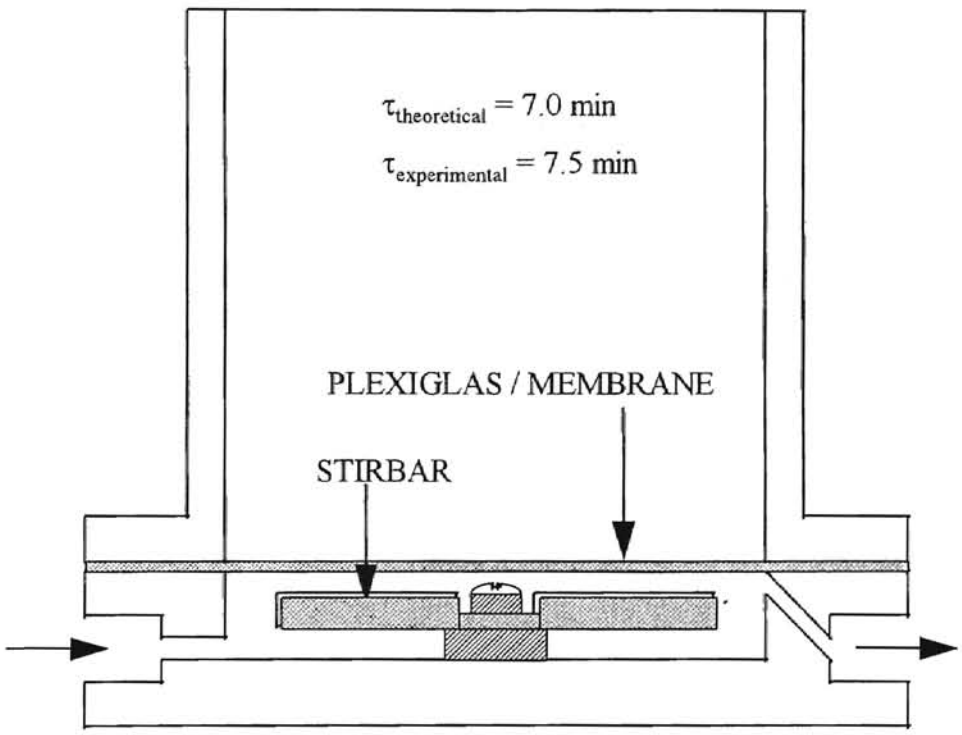

Figure 3.2. Stirred vessel (see text for dimensions).

six million since it is not possible to perfectly plate the cells in a monolayer adjacent to each other. The height of the vessel is 0.8 cm to account for a 0.3 cm clearance between the stirbar and the bottom of the vessel, a 0.3 cm thickness of the stirbar fabricated from magnetic stainless steel (SS 416), and a clearance of 0.2 cm between the stirbar and the top of the vessel. The stirbar is 4.4 cm long × 0.6 cm wide and is held in place on a small projection from the base of the vessel by a teflon washer and nylon screw. A chamber provided above the vessel is separated from the stirred lower chamber by a circular 0.2 cm thick plexiglas sheet. For future experiments studying the effect of macrophages and their products on β-cells, the two chambers will be separated by a semi-permeable membrane. The stirred vessel is provided with two diametrically opposite holes which function as the inlet and outlet for the liquid. The outlet is located near the top of the vessel while the inlet is located at the bottom. This facilitates the elimination of air from the chamber during liquid filling. The volume of the vessel and the 1/8 inch Swagelok® fittings at the inlet and the outlet is ~21.0 ml. Therefore, the theoretical residence time is 7.0 min for a flowrate of 3.0 ml/min.

3.4.4 Design evaluation.

A residence time distribution (RTD) study was undertaken to determine how well the vessel approximated an ideal CSTR. Methylene blue (Aldrich Chemical Company, WI, USA) was used as the tracer. The vessel was evaluated at flowrates of 3 and 6 ml/min and stir speeds of 20, 30 and 40 rpm. A pulse of dye was injected at the inlet and the absorbance at 652 nm was measured with time using a spectrophotometer (Model UV-1601, Shimadzu Scientific Instruments, Inc., Maryland, USA) The point of measurement

and the outlet of the stirred vessel were separated by 60 cm of 0.32 cm OD teflon tubing (residence time 0.4 min).

As shown in Figure 3.3, the curve of absorbance vs time decayed exponentially after initially attaining a maximum value. For an ideal CSTR, the concentration can be expressed as a function of time and initial concentration such that

$$C = C_0 e^{-\frac{t}{\tau}} \tag{3.1}$$

Equation 3.1 may also be written as

$$\ln C = \ln C_0 - \frac{t}{\tau} \tag{3.2}$$

Since the absorbance is proportional to the concentration of tracer, the residence time of the vessel was determined by fitting the absorbance vs time data to Equation 3.2 (see Figure 3.4). The average residence times at 20, 30, and 40 rpm were 7.37±0.42, 7.43±0.42, and 7.66±0.15 min, respectively. Therefore, there was no significant difference between the residence times at these stirring speeds. It was decided to use 30 rpm for the stir speed as it seemed to provide adequate mixing without subjecting the cells to too much shear. The mean residence times for flowrates of 3.0 and 6.0 ml/min, irrespective of the stir speed, were 7.47±0.37 and 3.43±0.19, respectively. The mean residence time for a flow of 6.0 ml/min was 10% lower than half the corresponding value for a flow of 3.0 ml/min and is approximately equal to the theoretical residence time for a flow of 6.0 ml/min.

The vessel was recently modified by increasing its depth to 9.5 mm as compared to the earlier 8 mm. The new volume of the vessel is 25.0 ml. This corresponds to a theoretical

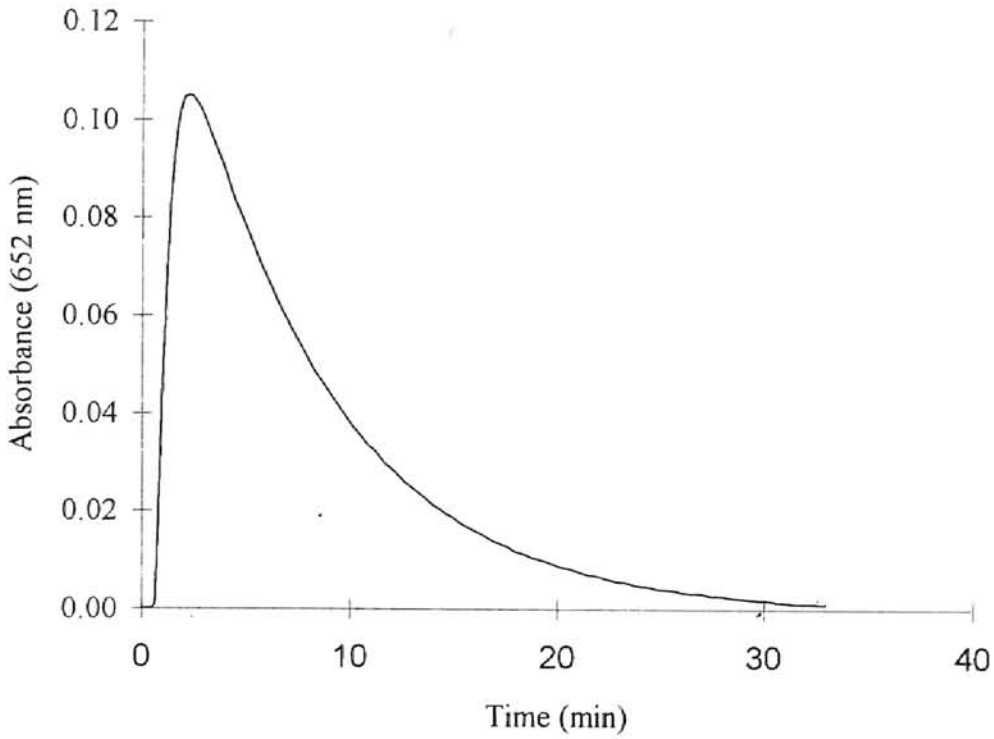

Figure 3.3. Residence time distribution curve of stirred vessel. The flowrate is 3.0 ml/min with stirring at 30 rpm.

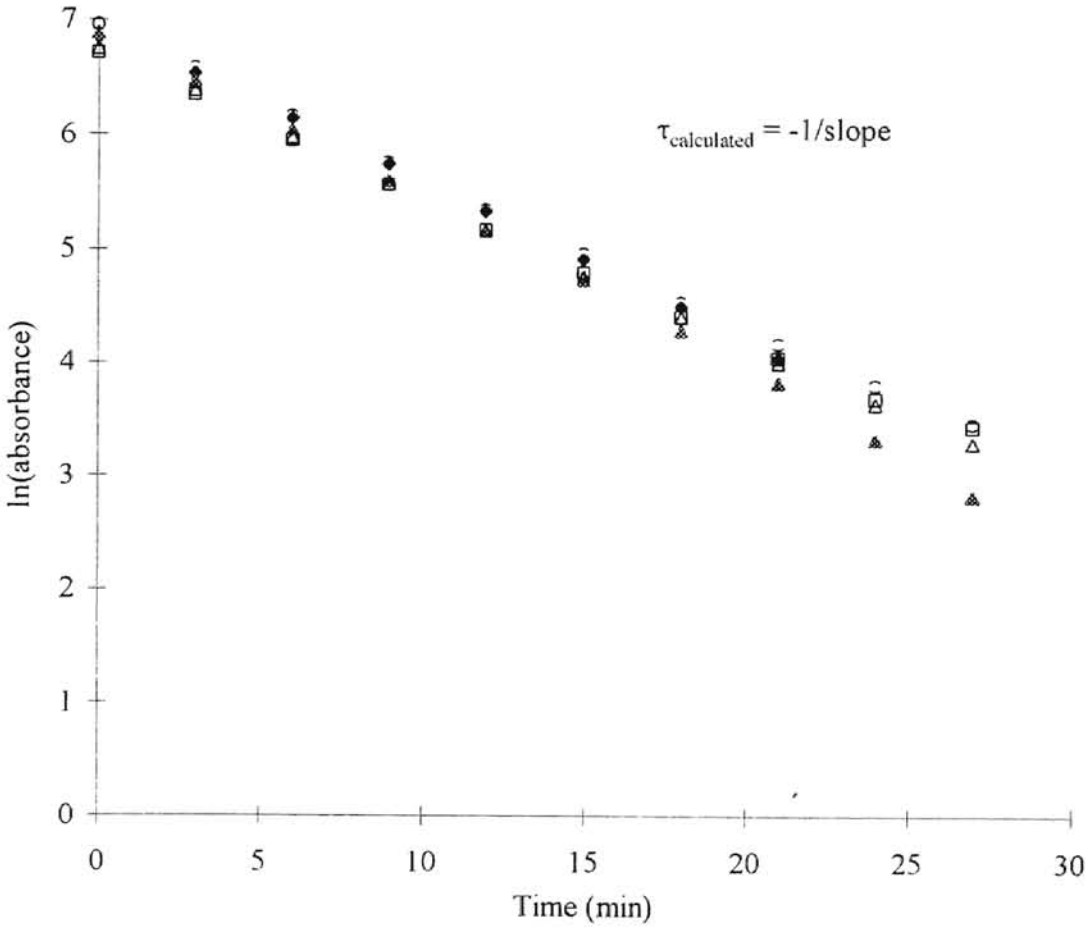

Figure 3.4. Residence time plot. The flow rate is 3.0 ml/min and the stir speed is 30 rpm in each experiment

residence time of 8.3 min at a flowrate of 3.0 ml/min. Experiments using a step change in dye concentration at the vessel inlet were then performed to determine its residence time and to determine the reason for the earlier observed differences in the theoretical and experimental residence times. The concentration of the dye was measured in a spectrophotometer at a point separated from the vessel outlet by 56 cm of 0.32 cm O.D. teflon tubing. For a flowrate of 3.0 ml/min the residence time of this tube is 0.4 min as determined using the 0.16 cm inner diameter. The absorbance vs time data from the experiments was used to determine the collective residence time of the vessel and the teflon tube. The total residence time is given by

$$\tau = \frac{\sum t_j C_j}{\sum C_j} \tag{3.3}$$

where all the absorbance data (C) from the beginning (t = 0) up to the time taken to achieve steady state is used in Equation 3.3.

The total experimental residence time is 8.5±0.4 min. For systems in series, the total residence time is the sum of the residence time of each system. Therefore, subtracting the tube residence time of 0.4 min from the total experimental residence time yields a vessel residence time of 8.1 min. This is in excellent agreement with the theoretical vessel residence time of 8.3 min. However, the residence time determined by fitting the absorbance decay data to Equation 3.2 is 8.8±0.7 min. The discrepancy between this value and the vessel theoretical value is likely explained by the fact that the exponential data represents not only the vessel behavior but also the tube behavior. If the tube does not represent a perfect plug flow then the vessel residence time will be convoluted,

causing the experimental residence time to be greater than the corresponding theoretical value of the vessel. This is likely the reason why analysis of data obtained using a pulse input gave an experimental residence time greater than the theoretical vessel residence time. A likely reason the data for a flowrate of 6.0 ml/min gave a measured residence time value that is in good agreement with the theoretical residence time may be that the flow was more representative of plug flow at the higher flowrate as compared to the flowrate of 3.0 ml/min. In any case, since the vessel outlet concentration is likely to be affected by the radial position of a pulse injection residence time analysis, using a step change is more reliable.

The preceding observations together with the nature of the graph presented in Figure 3.3 lead to the conclusion that the originally designed vessel closely approximated an ideal CSTR. Economic considerations dictate the use of a flowrate of 3 ml/min. In addition, the theoretical residence time of 7.0 min is appropriate for use in the model and will be used in preference to the possibly inaccurate value of 7.5 min.

CHAPTER 4

MODELING NITRIC OXIDE DELIVERY

Modeling the mass transfer of NO to solution and its subsequent reactions in the stirred vessel with the dissolved oxygen constitutes an important step in achieving well defined NO delivery rates and concentration profiles. A validated model would enable achievement of the desired NO concentrations in the stirred vessel without resorting to experimental verification.

4.1 Modeling mass transfer of NO in the delivery device.

The rate of mass transfer of a species (i.e. NO) from gas to liquid across semi-permeable membranes that form the upper and lower sides of a rectangular duct containing the liquid has been predicted [Colton and Lowrie, 1981]. The model predictions are based on the assumptions of fully developed laminar flow, steady-state conditions, homogenous fluids, and the absence of aqueous mass transfer across the permeable membranes.

4.1.1 Model formulation.

The mass balance over a differential length, dz, of the delivery device (see Figure 4.1) representing plug flow is written as

$$-QdC = k_o(C - C_o)2wdz \qquad (4.1)$$

where z is the length, w is the width, and the concentration corresponding to the gas

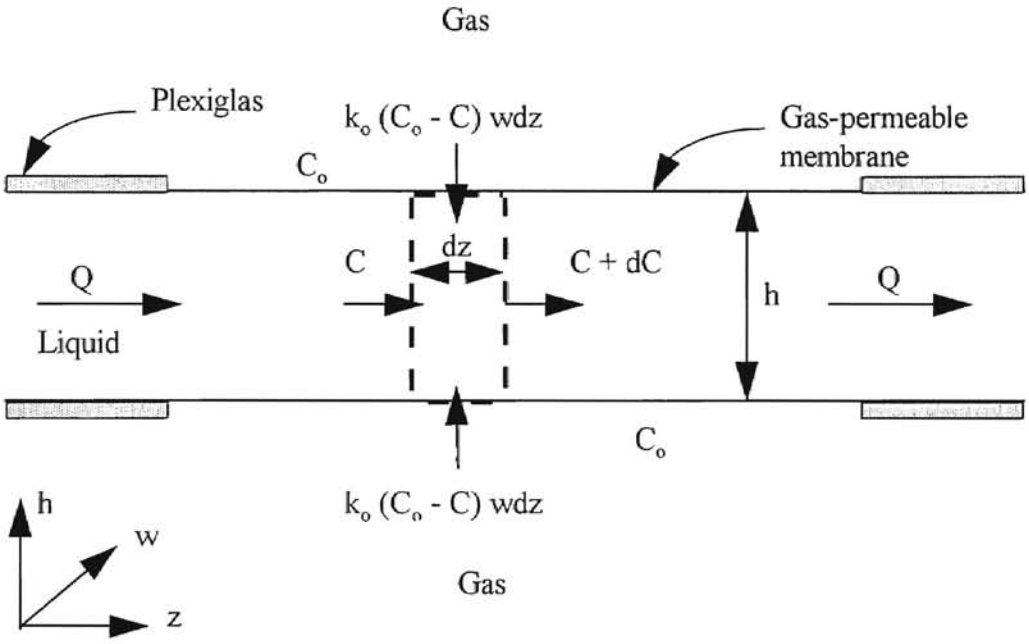

Figure 4.1. Mass balance analysis of delivery device.

partial pressure P_i is C_o. The relationship of C_o to P_i is $C_o = H P_i$, where H the Henry's law constant. Q is the liquid volumetric flowrate, k_o is the average overall mass transfer coefficient, and C is the concentration in the bulk liquid. Equation 4.1 is subject to the boundary conditions $C_m = 0$ at $z = 0$ and $C_m = C_{out}$ at $z = L$. Integration of Equation 4.1 yields

$$C_{out} = C_o(1 - e^{-2wL\frac{k_o}{Q}}) \tag{4.2}$$

The value of k_o is determined from the overall Sherwood number which is defined in terms of k_o, the aqueous diffusivity (D), and the distance separating the two membranes (h) such that

$$Sh_o = \frac{k_o h}{D} \tag{4.3}$$

Sh_o is representative of the dimensionless concentration gradient at the boundary layer and is indicative of the overall resistance to mass transfer (resistance $\propto 1/Sh_o$). Analogous to electrical circuits where resistances in series are added to give the total resistance, the resistances of the permeable membrane and the adjacent liquid boundary layer are added to yield the overall resistance to mass transfer. Therefore, the overall Sherwood number is related to the Sherwood numbers for the membrane wall (Sh_w) and liquid boundary layer (Sh_f) by

$$\frac{1}{Sh_o} = \frac{1}{Sh_w} + \frac{1}{Sh_f} \tag{4.4}$$

The wall Sherwood number is similarly defined as $Sh_w = \frac{k_w h}{D}$ where k_w is the mass transfer coefficient characterizing mass transport through the wall. Using the permeability P^* of the Silastic® membrane, k_w is expressed as

$$k_w = \frac{1000P^*}{H\delta} \tag{4.5}$$

where P^* is in mol cm^{-1} s^{-1} $cmHg^{-1}$, H is in M $cmHg^{-1}$, and δ, the thickness of the membrane, is in cm. Thus,

$$Sh_w = \frac{1000P^*h}{H\delta} \tag{4.6}$$

Using the model of Colton and Lowrie [1981], Sh_f is determined from Sh_w, the membrane length (L), the diffusivity (D), the average velocity ($\bar{v}$), and the membrane separation height (h). Assuming that a negligible amount of NO reacts between its point of entry into the liquid and the outlet of the delivery device, the NO concentration (C_{out}) at the outlet of the delivery device is determined using Equation 4.2.

4.1.2 Sherwood numbers.

The values of the aqueous diffusivity, Henry's constant, and membrane permeability for NO at 25°C are 2.7×10^{-5} cm^2 s^{-1}, 2.5×10^{-5} M $cmHg^{-1}$, and 2.3×10^{-12} mol cm^{-1} s^{-1} $cmHg^{-1}$, respectively, whereas at 37°C, the corresponding values are 5.1×10^{-5} cm^2 s^{-1}, 2.1×10^{-5} M $cmHg^{-1}$, 5×10^{12} mol cm^{-1} s^{-1} $cmHg^{-1}$, respectively [Lewis, 1994]. The permeability at 37°C is approximately twice the reported value at that temperature, in order to account for the effect of heating the Silastic® membrane during sterilization in an autoclave before use in experiments at 37°C [Lewis, 1994]. The values of L, w,and h are 2.5 cm, 0.5 cm, and 0.3 cm, at all temperatures, respectively. The average velocity over the cross-sectional area of the rectangular duct is 0.32 cm s^{-1} at a flow of 3.0 ml/min.

At 25°C, Sh_w is 84 and the model predicted Sh_f to be 11.5. This indicates that the liquid boundary layer resistance is approximately 7 times the wall resistance and is thus the controlling factor in the mass transfer of NO. Similarly, at 37°C the values of Sh_o, Sh_w and Sh_f are approximately 9, 120, and 10, respectively, again indicating a major role for the liquid boundary layer in controlling the aqueous NO concentration achieved at the outlet of the delivery device.

4.1.3 Model validation.

Experiments were performed at 25°C and 37°C to measure the NO concentration at the delivery device outlet for comparison with the model predictions.

4.1.3.1 Experimental setup.

A gaseous mixture of 10% NO and 90% nitrogen (H.P. Gas Products, Inc., Baytown, TX) was mixed with ultra high purity nitrogen (UHP N_2) (Sooner Airgas, Stillwater, OK) to achieve the required gaseous partial pressures. The 10% NO / N_2 mixture made it possible to achieve low partial pressures required to establish aqueous NO concentrations on the order of a few nM without excessive use of nitrogen. Flowmeters (Porter Instrument Co., Hatfield, PA, USA) with capacities of 10 sccm and 1000 sccm were used to control the flowrates of the NO/N_2 mixture and UHP N_2, respectively. Before conducting any experiments, the flowmeters were calibrated using a bubble flowmeter. Both the flowmeters permitted flow that was higher than the set value by 5-7%. The ratio of actual flow to the setpoint was 1.066 for the NO/N_2 flowmeter whereas it was 1.053 for the UHP N_2 flowmeter. A check valve (OKC Valve and Fitting Co., Oklahoma City,

OK) having a crack pressure of 0.3 psi was used in the NO/N_2 gas line immediately following the flowmeter in order to prevent backflow. In the UHP N_2 line, an O_2 gas purifier (Model DGP-125-R1, VWR Scientific, CA, USA) was introduced before the flowmeter to completely remove oxygen and preclude any formation (by oxidation of NO in the gas phase) of nitrogen dioxide (NO_2) that could diffuse into the liquid and form reaction products that were detrimental to the function of cells. To ensure complete removal of NO_2 following mixing, the gas was bubbled through a solution of 4M sodium hydroxide (NaOH). The experimental setup is shown in Figure 4.2.

The liquid flowing through the delivery device consisted of 0.01 M phosphate buffer (pH 7.4). The buffer was contained in a 1 liter conical flask open to the atmosphere and was stirred vigorously using a teflon coated stirbar to saturate the solution with oxygen. The solution was pumped to the delivery device by a peristaltic pump that used teflon tubing (Masterflex®, Model 77390-00, Cole-Parmer Instrument Co., IL, USA). When performing experiments at 37°C, the flask was partially immersed in a water bath maintained at 38°C (to compensate for heat losses during flow) by an immersion circulator (Model 71, VWR Scientific Products).

The NO concentration was measured at the delivery device outlet using an amperometric probe (ISO-NOP, World Precision Instruments, Sarasota, FL, USA) having a measurement sensitivity of 1 nM. The probe has a membrane covering a platinum electrode where oxidation of NO generates current. The electrode is enclosed by a slender steel body which is inserted into a luer lock adapter that fits securely on a tee luer fitting. The tee luer was attached to the teflon tubes (0.32 cm O.D.) that conveyed

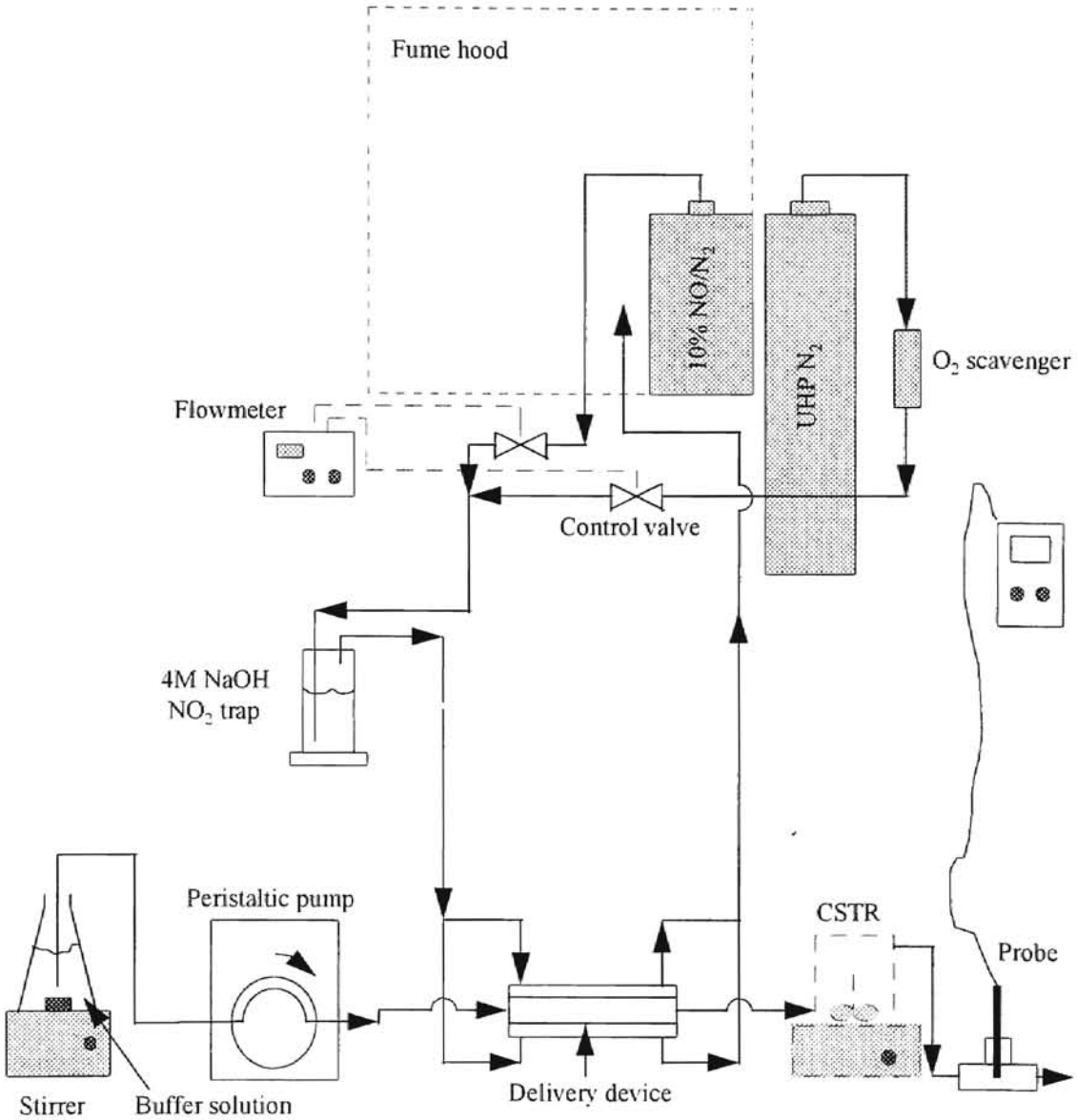

Figure 4.2. Experimental apparatus.

the NO solution to and from the tee. The current value of the probe response was displayed by a battery powered meter and recorded by an integrator (Model HP 3395, Hewlett Packard Co., USA). Experiments at 37°C required the delivery device and probe to be located inside an incubator (Model 1510E, VWR Scientific, CA). In addition two holes were drilled in the sides of the incubator to provide convenient entry and exit points for the tubes conveying the liquid. All the tubing used in the experimental setup, except where specified, was 0.32 cm O.D. teflon tubing while all the tube fittings were stainless steel.

4.1.3.2 NO calibration procedure.

The NO probe was calibrated prior to measuring NO concentrations. This was achieved by recording the electric current values corresponding to known NO concentrations. At 25°C, known concentrations of NO were generated by bubbling gas through buffer solution contained in a 125 ml conical flask. The solution was deoxygenated prior to calibration by bubbling UHP N_2 for 1 hour. After deoxygenation different NO saturation concentrations were achieved by varying the partial pressure of NO and quantifying the NO concentration from NO solubility data [Lange, 1967]. The saturated solution was pumped at 3.0 ml/min through a closed loop containing the NO probe and the pump. The values of the electric current (nA) generated at NO concentrations of 0.31, 0.61, and 0.92 μM, obtained with NO partial pressures of 1.52×10^{-3}, 3.03×10^{-3}, and 4.55×10^{-3} atm, respectively, were recorded to arrive at the calibration curve. The probe response in the absence of aqueous NO was used as the baseline value.

At 37°C the calibration was performed by bubbling NO containing gas through buffer in a one liter flask placed in the water bath. However, the same partial pressures of NO that were used at 25°C resulted in NO concentrations of 0.25, 0.50 and 0.75 μM due to a reduction in NO solubility at 37°C. The probe was placed inside the incubator maintained at 37°C while the NO solution was pumped at 3.0 ml/min to the probe. Unlike at 25°C, the NO concentration was not recycled.

4.1.3.3 Experimental procedure.

Experiments at 25°C and 37°C followed different procedures due to the extreme temperature sensitivity of the NO probe. The probe is sensitive to temperature variations and temperature changes as small as 0.05°C change the current output. The probe was stored in a vial containing deionized water when not in use for short periods of time (less than a week), such as in between experiments. This regenerates the electrode in the probe by removing the NO molecules adjacent to it.

Experiments at 25°C were initiated by priming the pump with buffer solution. Immediately after this, the delivery device was filled by holding it in a vertical position to ensure removal of all the air bubbles. A short piece of teflon tubing, attached at one end to a short tygon tube linked to a luer fitting, was used to connect the delivery device outlet to the tee that would hold the probe. The probe was inserted into the tee only after liquid began flowing from the open arm of the tee. This was done to eliminate air bubbles within the tee. The remaining arm of the tee was left open so that the liquid dripped into an open trough. It is important to note that the probe, being extremely pressure sensitive, gave a higher response when placed in flow as compared to the response in stagnant liquid due to

the higher hydrostatic pressure in flowing liquid. The flow setting was adjusted to give 3.0 ml/min of flow as verified by flow measurement using a graduated cylinder. This was important as even a slightly different flow changed the probe response due to an increase or decrease in the hydrostatic pressure experienced by the probe.

The probe was used to validate the NO concentration values predicted by the model (Equation 4.2) at NO partial pressures of 1.25×10^{-3}, 2.51×10^{-3}, 5.00×10^{-3}, and 10.00×10^{-3} atm using UHP N_2 and NO/N_2 mixture flowrate combinations of 99.0 and 1.25 sccm, 97.0 and 2.5 sccm, 95.0 and 5.0 sccm, and 90.0 and 10.0 sccm, respectively. After adjusting the liquid flowrate to 3.0 ml/min, the UHP N_2 flow was turned on and set to the appropriate flowrate. The probe response was allowed to reach steady-state. The NO/N_2 gas was then turned on and set to the appropriate flowrate. When the probe response reached a steady value, it was recorded and the UHP N_2 and NO/N_2 mixture flowrates were adjusted to values corresponding to the next higher NO partial pressure. This was repeated until readings for all the NO partial pressures had been obtained. The NO/N_2 mixture flow was then turned off while leaving the UHP N_2 flow on for a few minutes in order to sweep away all the residual NO from the delivery device. After turning off the liquid flow, the probe was removed from the tee and its tip washed with deionized water before returning it to the vial containing deionized water for storage.

At 37°C the experimental procedure was initiated with the connection of the pump to the delivery device inlet. The pump was then primed and the delivery device was filled with the warm buffer solution. All of the tubing, whether inside the incubator or outside, was insulated with fiber glass. The body of the probe was also insulated. This was done

to dampen the effect of the slight changes in temperature inside the incubator on the probe response. After the delivery device was filled, the probe was inserted into the tee as explained previously. Once the probe was set up, the incubator door was closed until the experiment ended. The flow was then set to 3.0 ml/min.

At 37°C, the heating-cooling cycle of the incubator played an important role. The incubator turned on the heat for about 1.5 minutes approximately once every 20 minutes. The heating was followed by a period of cooling of about 18 minutes. The effect of heating on the probe response became evident when the heating stopped. The response increased over the next 9 to 10 minutes by about 0.10 nA and then stayed nearly constant for about 2 minutes before beginning to decrease. The response decreased by about 0.08 to 0.09 nA (slowly in the beginning) during the next 4 to 5 minutes and continued to drop even when the heating turned on again. Fortunately, since the time taken for the NO concentration (or current) to reach steady-state was about 5 to 7 minutes, it was possible to observe the cycle of this increase/decrease in response due to heating/cooling and start the NO gas flow through the delivery device ~30 seconds before the response peaked. This meant the response could achieve steady-state before the cooling caused a significant decrease in the value. The steady-state response was noted and the NO/N_2 mixture was then turned off. This procedure was repeated for each NO exposure. Thus, the probe response for each NO exposure was determined using a slightly different baseline or reference value and was properly accounted for. The NO partial pressures were the same as those used at 25°C.

4.1.3.4 Results.

Calibration of the probe at 25°C yielded a linear current output (nA) vs NO concentration profile having slopes ranging from 0.80 to 0.95 nA/μM. At 37°C slopes of the calibration curves were in the range of 0.95 to 1.20 nA/μM (see Figures 4.3 and 4.4). Figures 4.5 and 4.6 show the experimental outlet NO concentrations as well as the outlet concentrations predicted by the model. At 25°C the measured values deviated from the model predictions by ± 7% or lower. At 37°C, the deviation was ± 12% in the concentration corresponding to the highest partial pressure of 10.00×10^{-3} atm and ± 7% or lower in the concentrations corresponding to the other three partial pressures. It is likely that the greater error in the highest concentration response at 37°C is due to the temperature sensitivity of the NO probe response.

Figure 4.7 compares the NO concentration predictions at the delivery device outlet for flowrates of 2.7, 3.0, and 3.3 ml/min. Small changes in the liquid flowrate cause a small change in the rate of mass transport of NO. At 2.7 ml/min, the NO concentration values at all NO partial pressures are higher by 5.5% while at 3.3.0 ml/min they are 7% lower as compared to corresponding values at 3.0 ml/min.

4.2 Modeling the NO concentration in the CSTR.

The CSTR designed to contain the β-cells was connected to the outlet of the delivery device using a 15.5 cm long piece of 0.32 cm O.D. teflon tubing. The tubing between the delivery device and the CSTR was modeled as a plug flow reactor (PFR) where the PFR outlet NO concentration is the inlet NO concentration for the CSTR. For a well-stirred

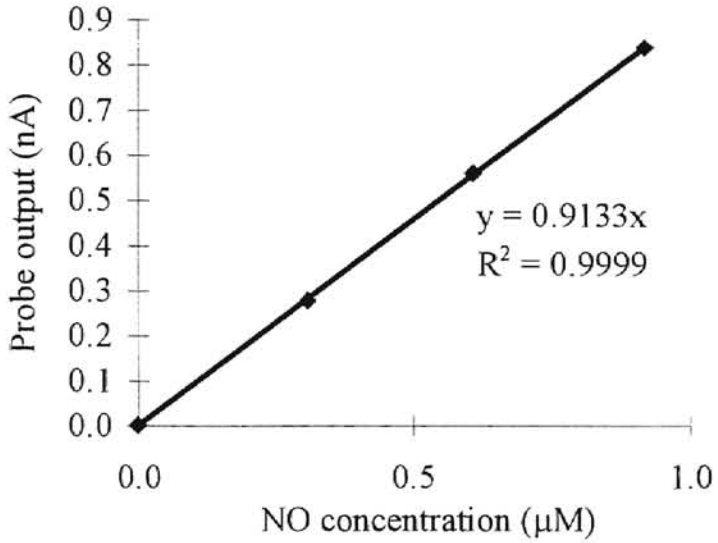

Figure 4.3. NO probe calibration curve at 25°C.

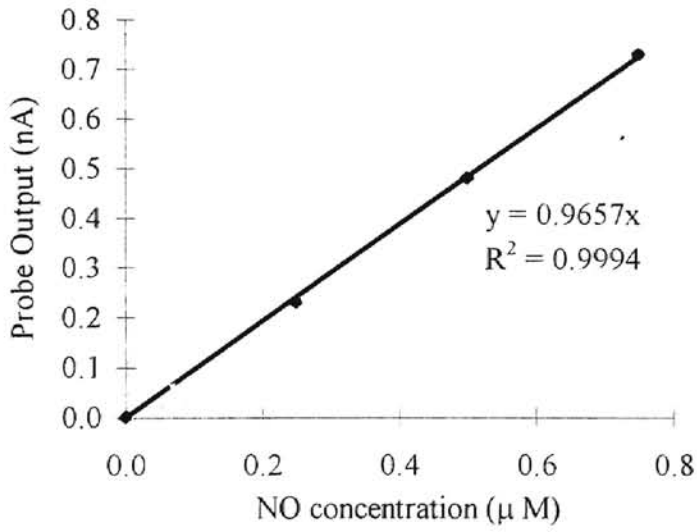

Figure 4.4. NO probe calibration curve at 37°C.

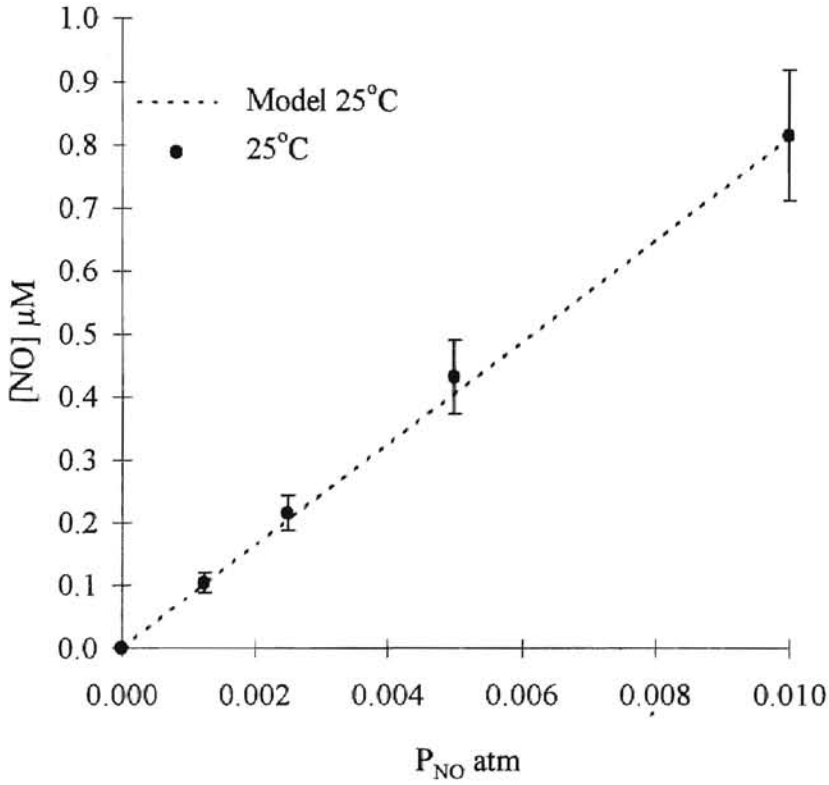

Figure 4.5. NO concentration predictions and experimental results of delivery device at 25°C (n = 6 experiments).

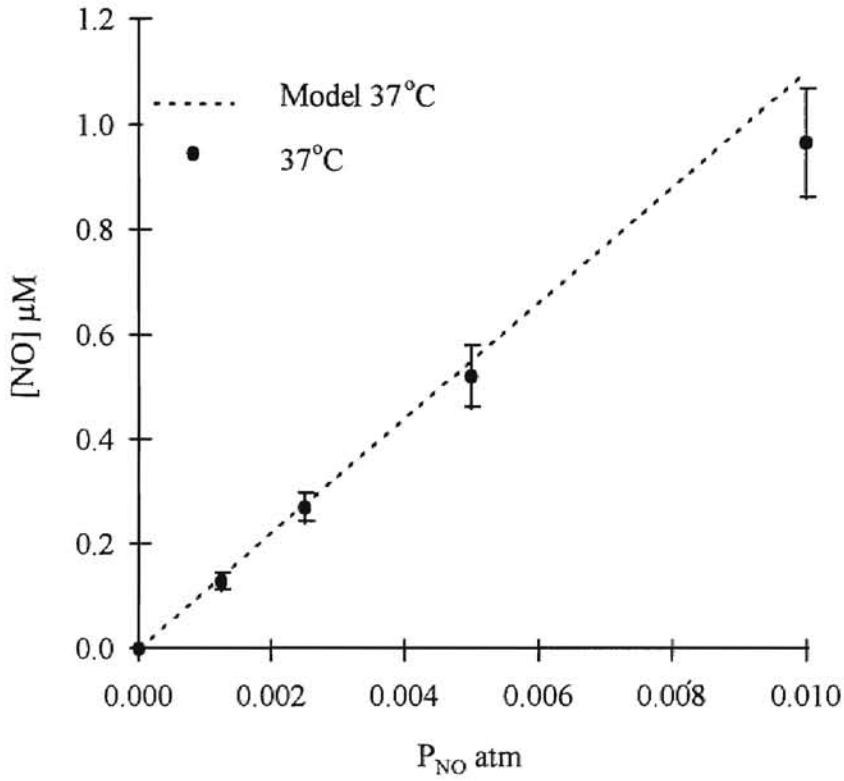

Figure 4.6. NO concentration predictions and experimental results of delivery device at 37°C (n = 4 experiments).

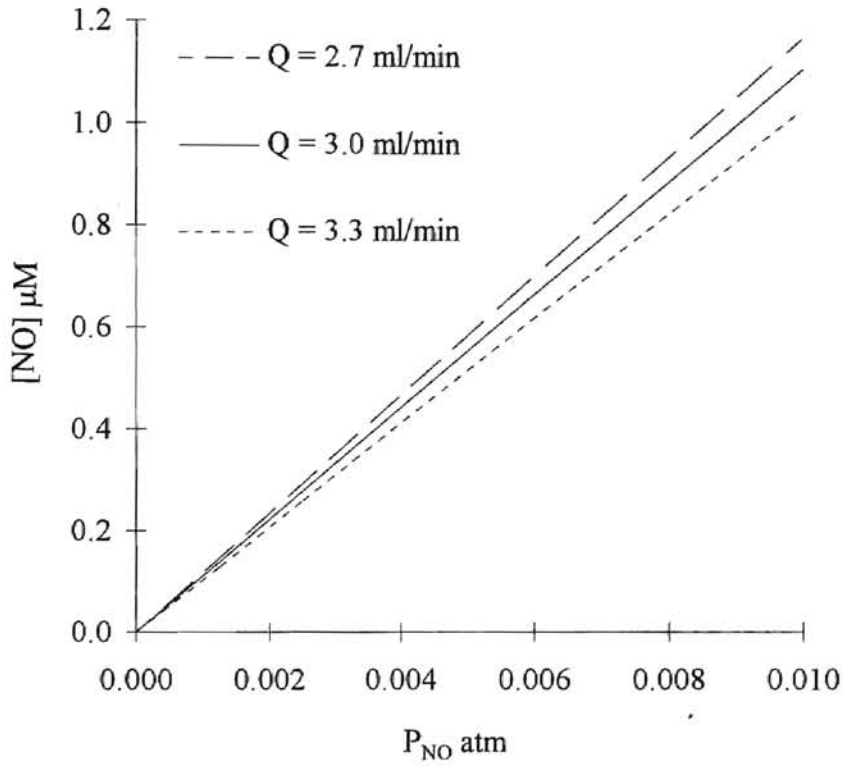

Figure 4.7. Effect of flowrate (Q) on model predictions.

vessel, the NO concentration at the outlet is the NO concentration to which the cells are exposed.

4.2.1 The model.

The outlet NO concentration predicted for the delivery device is used as the inlet concentration for the PFR. A mass balance over a differential length of the PFR yields

$$dC = R_{NO} d\tau \tag{4.8}$$

where τ is the average residence time $z / \bar{v}$. The rate of the aqueous reaction between NO and O_2 is given by the equation

$$R_{NO} = -4k_1 C_{NO}^2 C_{O_2} \tag{4.9}$$

The rate constant k_1 is 2.1×10^{-6} and 2.4×10^{-6} $M^{-2}s^{-1}$ at 25°C and 37°C, respectively [Lewis and Deen, 1994]. The saturated aqueous O_2 concentrations at those temperatures when exposed to air are 265 and 223 μM, respectively [Lewis, 1995]. Integration of Equation 4.8 using boundary conditions $C = C_{out}$ at $\tau = 0$ and $C = C_{pfr}$ at $\tau = \tau_{pfr}$ yields

$$C_{pfr} = \left(\frac{1}{C_{out}} - 4k_1 C_{O_2} \tau_{pfr}\right)^{-1} \tag{4.10}$$

The assumption made in the integration is that the oxygen concentration in the liquid remains unchanged at its saturation value for the given temperature. This is justified as the NO concentration in the liquid is less than 1% of the aqueous O_2 saturation concentration and NO reacts in the stoichiometric ratio 4:1. The residence time (τ_{pfr}) in the short tube connecting the delivery device to the CSTR is 0.1 min based on the 0.16 cm inner diameter of the tube, a length of 15.0 cm and a flowrate of 3.0 ml/min. Considering the concentration computed from Equation 4.10 to be the inlet NO concentration for the

CSTR, the NO concentration at the outlet of the CSTR (C_{cstr}) is determined using a simple mass balance

$$C_{cstr} = C_{pfr} - 4k_1 C_{cstr}^2 C_{O_2} \tau_{cstr} \tag{4.11}$$

Equation 4.11 was solved to yield

$$C_{cstr} = \frac{\sqrt{1 + 16k_1 C_{O_2} \tau_{cstr} C_{pfr}} - 1}{8k_1 C_{O_2} \tau_{cstr}} \tag{4.12}$$

where τ_{cstr} (= 7.0 min) is the residence time in the CSTR.

4.2.2 Experimental setup and procedure.

The experimental setup was the same as earlier described in section 4.1.3.1 with the addition of the CSTR at the delivery device outlet. The CSTR was placed on a stir plate (Micro Stir model II, Wheaton Instruments, NJ, USA) which operated at 30 rpm (see Figure 4.2). For experiments at 37°C, the CSTR and the stir plate were kept inside the incubator with the delivery device, and the NO probe was connected to the outlet of the CSTR to measure the NO concentration of the CSTR.

The experiments at both temperatures were initiated as explained in section 4.1.3.3. The only difference was that the CSTR and delivery device were not connected until the delivery device had been filled. The CSTR was filled by tilting it slightly so that the outlet was the highest point inside the CSTR. This facilitated the removal of all the air from the CSTR. The NO probe was then inserted in the CSTR outlet tubing.

For experiments at 25°C, after recording the baseline reading, the NO/N_2 mixture flow was turned on and set to obtain a partial pressure of 1.25×10^{-3} atm. Steady-state was achieved in about 30 minutes. Once the probe response for the partial pressure of NO had

been recorded, the experiment proceeded to the next higher partial pressure. This carried on until the readings for all the same partial pressures used earlier (Section 4.1.3.3) had been obtained. In some cases, the above procedure of measuring NO concentration requiring the probe to be continuously exposed to NO for about two hours caused the electrode of the probe to become saturated with NO. This affected the readings, so a modified procedure was adopted. In this new procedure, the experiment was be begun by recording the baseline value of probe current output, followed by disconnection of the tee containing the probe from the CSTR. The probe was maintained in this condition for the next half hour while the NO concentration achieved steady state. The probe was then reattached to the CSTR and the response was recorded. Following this, the tee was disconnected once again and the partial pressure of NO increased to the next higher value while the tee was flushed with deionized water. The probe remained in deionized water for the next half hour until it was time for the next reading. This procedure yielded satisfactory results but could not be used at 37°C as opening the incubator frequently caused large temperature changes that would affect the probe response.

At 37°C, the NO concentration measurements were made continuously with only one experiment being performed per day in order to allow the electrode to be refreshed by a sufficiently long period of cleansing in the deionized water. The procedure of measurement required knowledge of the increase and decrease in the NO response due to heating and cooling of the incubator. The flow of the NO/N_2 mixture was turned on just before the baseline response reached its peak. The NO concentration (probe current output at steady-state) was obtained when the current increased to its next peak value

which would usually be about 30 minutes from the time the NO flow was turned on. This procedure worked only because the rise and fall in the response during heating and cooling were the same or the difference was a negligible fraction of the response. However on cold days, the response cycled more frequently and with greater amplitude making it very difficult to achieve a well-defined steady-state probe response. This was, however, alleviated to a great extent by wrapping the CSTR in fiber glass insulation. In fact, avoiding direct contact between the CSTR or delivery device and other solid surfaces helped dampen the fluctuations in the probe response caused by temperature variations.

4.2.3 Results.

The results at 25°C and 37°C are shown in Figures 4.8 and 4.9. At 25°C, the measured values of NO concentration differed from the model predictions by ± 21% or less, whereas the NO concentrations measured at 37°C deviated by ± 7% or less from the model predictions. The residence time used for the CSTR predictions was 7.0 min. For a residence time of 7.5 min and a NO partial pressure of 0.01 atm, the model predicted NO concentrations that were only 2% lower than the corresponding predictions using a residence time of 7.0 min. This is not surprising given that the reaction is second order in NO concentration and the concentrations for this study are in the nanomolar range.

4.3 Problems encountered in the experiments.

Numerous problems were encountered with the probe, delivery device, peristaltic pump, and the stirbar in the CSTR. Some of these problems were remedied. This section

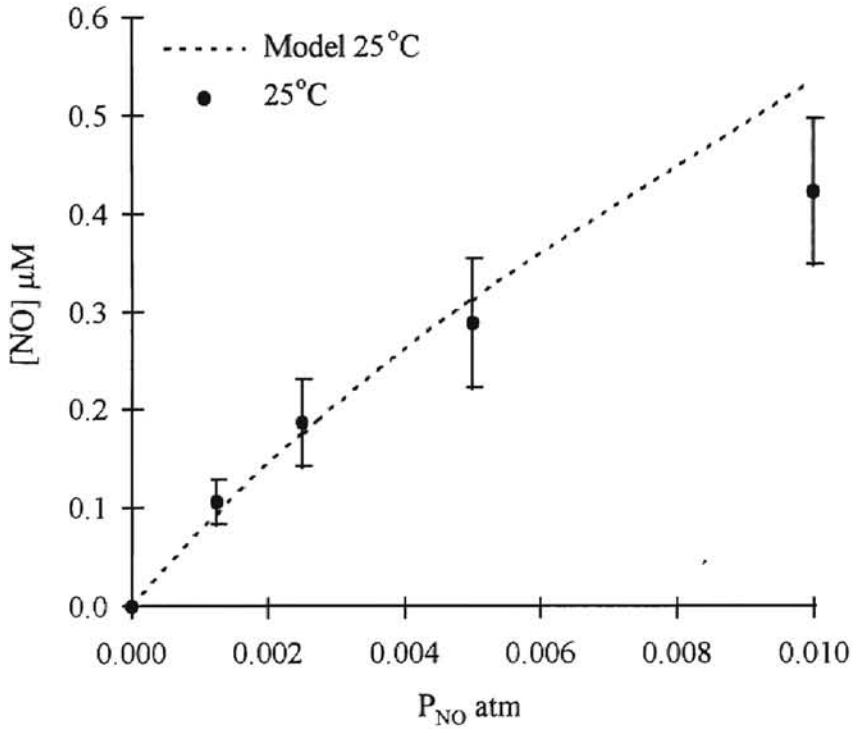

Figure 4.8. NO concentration predictions and experimental results of CSTR at 25°C (n = 5 experiments).

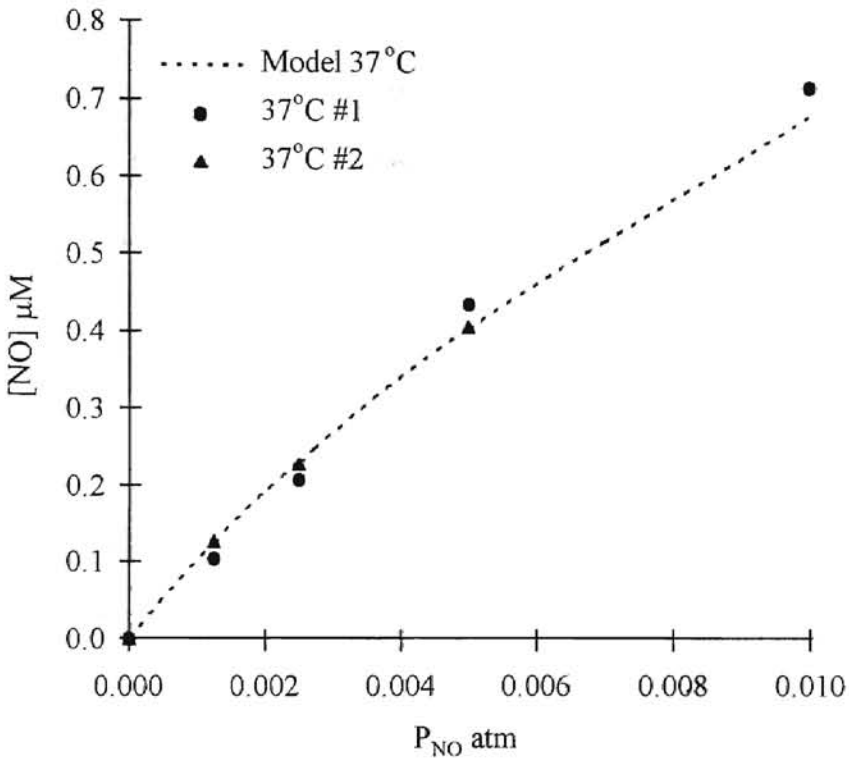

Figure 4.9. NO concentration predictions and experimental results of CSTR at 37°C.

describes the problems encountered in performing experiments at 25°C and 37°C and identifies the experimental uncertainties to be aware of when interpreting the results.

4.3.1 Problems with the NO probe.

Most of the problems encountered dealt with the probe. The electrode in the probe did not function properly when an o-ring was used. This o-ring was to be slid on to the sleeve of the probe to prevent the luer lock fitting from sliding off. However, the o-ring was not needed as the luer lock fitting fit tightly on the steel sleeve of the probe. In addition, the o-ring fit tightly on the probe and when positioned on a sensitive 0.5 cm long region at the tip of the probe it hampered normal function of the probe due to the pressure it exerted on the electrode. The o-ring in this position lowered the sensitivity of the probe by a significant amount. This was the first indication of the probe's pressure sensitivity, a fact corroborated by observations of changes in the probe response caused by introduction of the probe in a flowing stream of liquid. The response also changes when the flowrate is changed, although the flowrate change may be a mere 0.2 ml/min. The probe response was found to vary in direct proportion to the applied pressure.

The radial position of the probe tip in the tee also affected the response by about 15%. The response for the same partial pressure of NO was greatest near the walls of the tee and the least at the center. The tightness with which the luer lock fitting is connected to the tee also seems to affect the response. The tighter the fitting is locked onto the tee, the higher is the probe response. This change in the probe response may be due to an increase in pressure on the probe tip or due to a change in radial position of the probe tip in the tee.

The probe is also very highly temperature sensitive. Even a change in temperature as small as 0.05°C can change the probe response. This has been noticed in experiments at 37°C where the probe response was found to increase and decrease with rise or fall in temperature even though the incubator controls the temperature to within ± 0.3°C. In addition, although the probe apparently is able to measure NO concentrations as high as 20.0 μM, the electrode gets saturated with NO when exposed to concentrations above 1.0 μM for more than ~45 minutes. There is an immediate and sharp decrease in the sensitivity of measurement upon saturation and the probe response falls. Finally, the presence of bubbles in the liquid also adversely affects the experiment. The bubbles cause the probe response to jump wildly. Conversely, if sudden inexplicable spikes in the response occur then it strongly indicates the presence of bubbles in the liquid.

When functioning properly, the probe should have a sensitivity in the range 0.5-1.0 nA/μM. The sensitivity should always be greater than 0.5 and the closer the sensitivity is to 1.0 nA/μM the better the condition of the probe. The probe is a very sensitive instrument that needs patient and careful handling to perform reliably for a long period of time. If the response is seen to slowly drift higher with time even in the absence of NO, there may be a microscopic hole in the membrane covering the electrode and the sleeve needs to be replaced. However, this behavior may also be due to a variation in the temperature of the liquid. Although the probe has many problems, it is a convenient instrument for measuring nanomolar concentrations of NO. The probe can be used to produce reliable results as demonstrated in this thesis.

4.3.2 Problems with the delivery device.

Another potential source of problems was the delivery device. In the beginning, it was noticed that the membrane was getting distended due to the pressure applied by the gas. The gas was constrained to leave the chamber via an outlet that was the same diameter as the inlet. The distention in the membrane increased the area available for mass transfer resulting in measured NO concentrations that were 1.5-2 times the values predicted by the model. This situation was remedied by doubling the diameter of the gas outlets. The way the device is filled also affects its performance. The presence of air bubbles on the membrane where the mass transfer takes place largely reduces the mass transfer to the liquid. The drop in NO concentration may be as much as 80% of the model NO concentration predictions. The best way to fill the delivery device is to hold it vertical so that the displaced air can leave easily.

4.3.3 Problems with the pump and stirbar.

Some relatively minor problems were caused by the peristaltic pump and the stirbar in the CSTR. The pump uses teflon tubing and unless the tubing tightly fits over the rollers, the flow will vary as the free end of the tube carrying the liquid is raised or lowered. This is because the hydrostatic pressure head acting on the liquid changes as the tube is raised or lowered causing the flow to vary. This problem is eliminated by ensuring that the tube inside the pump presses tightly against the rollers, otherwise the change in flow will change the probe response.

The problem with the stirbar was that, although it was made of stainless steel, it was not heat hardened and prolonged exposure to oxygen rich buffer tarnished the surface. In

addition, the stirbar appeared to react with the NO in the CSTR, affecting experimental measurements. Reaction with the stirbar can decrease the NO concentration by as much as 80% when compared to the predicted values. To remedy this, the stir bar was electroplated with gold to prevent reaction. However this thin layer of gold began to wear off in places subjected to frictional contact with the body of the CSTR. The stirbar was found to rust badly when exposed to Krebs-Ringer buffer solution used in experiments with cells. Therefore, a new stirbar design has been proposed. This stirbar will consist of a block of teflon provided with a longitudinal hole containing a bar magnet. The hole will be sealed with silicone adhesive to prevent the magnet from reacting with NO. The use of a screw and washer will be obviated by providing the stirbar with an integral cylindrical projection that fits into the hole provided for the screw in the CSTR. This projection will not only act as a pivot but also prevent changes in the position of the stirbar when the CSTR is tilted during filling.

4.4 Conclusions.

The results are extremely satisfactory considering the sensitivity of the measuring instrument and the low concentrations utilized. The model can be used to predict the NO concentration in the CSTR with an accuracy of ± 7% or less at 37°C. There may be no sharp threshold concentration beyond which the function of β-cells is hampered. However, there will likely be a species dependent range of NO concentrations and other specific criteria, such as time of exposure, that would be needed to be achieved before cellular dysfunction occurs. The results presented in the preceding sections amply qualify

the model to be a useful instrument in reliably achieving desired aqueous NO concentration exposures to cells.

CHAPTER 5

INVESTIGATING THE EFFECT OF NITRIC OXIDE ON β-CELLS

Preliminary experiments were conducted by exposing β-cells to NO in order to test the feasibility of using the designed experimental apparatus. Cells of the insulin secreting tumor cell-line INS-1 [Asfari et al., 1992] were used for the trial runs. Liquid samples containing insulin were collected from cell experiments and assayed to determine the effect of NO on insulin secretion.

5.1 Materials and methods.

RPMI-1640 without sodium bicarbonate but containing 11 mM glucose, donor calf serum, 2-mercaptoethanol, HEPES, penicillin-streptomycin, and trypsin EDTA were purchased from Life Technologies, Inc. (Grand Island, NY). Sodium pyruvate, poly-L-ornithine, bovine serum albumin (BSA), and D-glucose were obtained form Sigma Chemical Co. (St. Louis, MO). Hexahydrated calcium chloride ($CaCl_2$), magnesium sulfate ($MgSO_4$), dibasic potassium phosphate (KH_2PO_4), and sodium chloride (NaCl) were purchased from Fisher Scientific (Fair Lawn, NJ). Sodium bicarbonate ($NaHCO_3$) and potassium chloride (KCl) were obtained from EM Science (Gibbstown, NJ).

5.1.1 Cell culture conditions.

Insulin secreting INS-1 cells obtained as a gift from Dr. Kim at Purdue University were

grown in culture medium consisting of RPMI-1640, 1 mM sodium pyruvate, 50 μM 2-mercaptoethanol, 10 mM HEPES, 2 g/liter $NaHCO_3$, 10% donor calf serum, and 1% penicillin-streptomycin.

The INS-1 cells were cultured in 100 mm culture dishes, passaged at ~80% confluency and incubated at 37°C in air containing 5% CO_2. The doubling time of the cells was ~3 days. It was noticed that the cells were infected with bacteria so 0.05 ml of gentomycin, obtained as a gift from Dr. Tim Burnham, Department of Microbiology, Oklahoma State University, was added to each culture dish to kill the infection. The bacteria decreased in number to a large extent but could not be completely eliminated. However, the cells were, still used in the trial experiments.

5.1.2 Preparation of cells for experiments.

For use in the experiments, cells were plated on 55 mm polycarbonate discs with a central hole of 10 mm diameter so as to fit in the CSTR. The discs were placed in 60 mm diameter lids of small glass culture dishes, attached to the bottom of the lid with two drops of silicone adhesive to prevent them from floating on the culture medium, and sterilized in an autoclave. Cell adhesion to the discs was facilitated by coating the discs with poly-L-ornithine using a 10 mg/liter solution of poly-L-ornithine in sterile water. This solution (5 ml) was allowed to stand in the lids containing the attached discs for 3 hours, following which the solution was removed and the lids washed twice with sterile water.

On the day prior to the experiment, the cells were detached from the 100 mm culture dishes by incubation with 0.05% trypsin-EDTA for 5 min. Culture medium (10 ml) was then added to the dishes following which the cell suspension was centrifuged at 1000 rpm

for 5 min. The supernatant liquid was discarded and the cells were resuspended in culture medium and plated on the discs at a concentration of ~5×10^6 cells per disc. The lids containing the dishes were then placed in the 100 mm culture dishes and incubated overnight so that the cells could attach to the discs.

5.1.3 Treatment of cells prior to the experiment.

An hour before the experiment, the culture medium was removed from the lids containing the discs, and replaced with ~7 ml of Krebs-Ringer-bicarbonate-HEPES buffer (KRBH), pH 7.4, containing 1 mM glucose. KRBH is composed of 134 mM NaCl, 3.5 mM KCl, 1.2 mM K_2HPO_4, 0.5 mM $MgSO_4$, 1.5 mM $CaCl_2$, 5 mM $NaHCO_3$, 10 mM HEPES, and 0.1% BSA. The cells were incubated at 37°C in this buffer for about one hour before transfer of the disc to the CSTR.

5.2 Experimental setup.

The experimental setup is shown in Figure 5.1. For the experiments, glucose free KRBH and KRBH + 20 mM glucose contained in two 1.0 liter bottles maintained at 37°C were used. The buffer solutions were gently stirred using two teflon coated stirbars rotated by a stirplate under the water bath. The lids of the bottles contained a hole ~5 mm in diameter. This hole was covered with a septum attached to the cap using silicone adhesive. Air containing 5% CO_2 was purged through the vapor space in the bottles using 3.8 cm long, sterile 20 gage needles provided with luer fittings. Two needles mounted on sterile 25 mm teflon filters, having a pore size of 0.2 μm (Cole-Parmer Instrument Co., Vernon Hills, IL), were used per bottle for gas inlet and outlet. The needles were

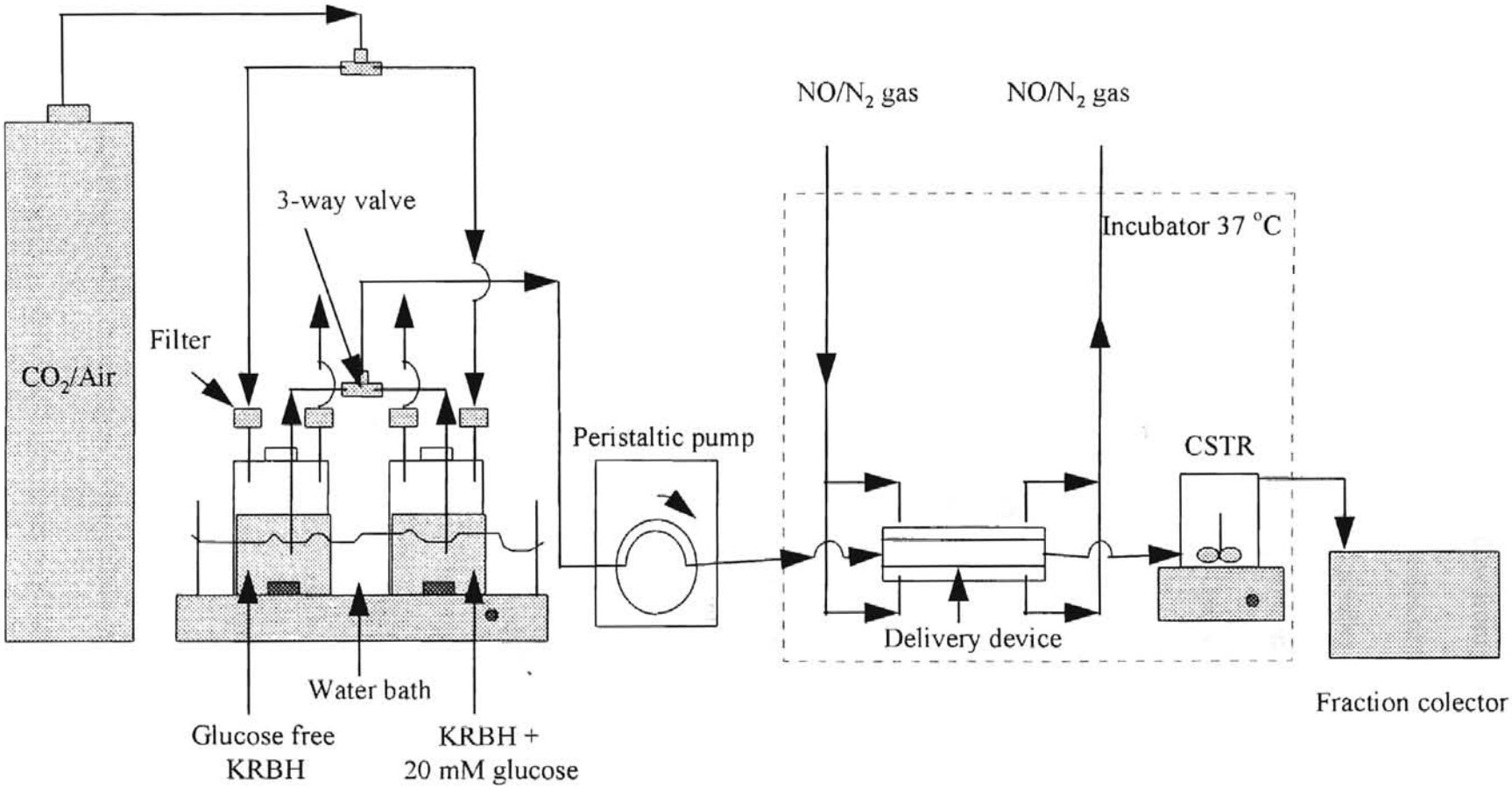

Figure 5.1. Experimental aparatus for cells.

inserted into the septa on the bottle caps. The gas flow from the CO_2/air tank was split using a tee and conveyed to the filters on the inlet needles of the two bottles by tygon tubing. Liquid was drawn from the bottles using two needles made from 0.16 cm O.D. stainless steel tubing. Both the needles conveying liquid from the bottles were attached to 0.32 cm O.D. teflon tubes connected to a teflon 3-way valve. The peristaltic pump was connected downstream of the 3-way valve using teflon tubing. The pump outlet was connected to the delivery device inlet while the delivery device outlet was connected to the CSTR inlet. The liquid from the CSTR outlet was collected in test tubes held in a fraction collector (Eldex Laboratories, Napa, CA).

5.3 Experimental procedure.

Before starting the experiment, the teflon tubing used in the peristaltic pump was connected to the needles inserted in the KRBH bottles and to the delivery device. The delivery device outlet and the needles were then covered with autoclave paper and the entire assembled unit was autoclaved. The CSTR was also autoclaved after separating the stirbar and screw and covering the inlet and outlet with autoclave paper. The stirbar and screw were wrapped separately in autoclave paper. The washer was not used in these experiments. The glucose free KRBH and the KRBH with 20 mM glucose were prepared earlier inside a sterile hood and stored at 4°C in sterilized bottles having caps without holes. The tubes and the tee conveying the gas were not sterilized as the microorganisms in the gas stream were kept out of the system by the filters.

The experiment began with replacement of the culture medium in the cell culture dishes with KRBH + 1 mM glucose, followed by incubation of these lids as explained earlier in

Section 5.1.3. Following this, sterile stirbars were added to the two bottles containing glucose free KRBH and KRBH + 20 mM glucose. The caps on the bottles were replaced by caps with septa. The four sterile 20 gage needles and the corresponding filters were connected and inserted into the septa, so that each bottle had a gas inlet and outlet. The filters were then connected to the tygon tubes, following which the bottles were transported with the entire assemblage and placed in the water bath. The stir plate was switched on and set to stir at a gentle speed to prevent frothing.

The CSTR was then opened inside the sterile hood and the disc containing the cells was placed in the CSTR. At the beginning of the experiment the discs were observed visually and the cells appeared well attached to the disc. However, the discs appeared only ~15% confluent (~ 1.5×10^6 cells) with little sign of any bacteria. KRBH was then added to the CSTR. The stirbar was put in place and the screw replaced. The top of the CSTR with the plexiglas plate was replaced and fastened to the lower portion of the CSTR. The CSTR was then connected to the delivery device. The entire assembly consisting of the 0.16 cm O.D. needles, the tubing inside the pump, the delivery device, the CSTR, and the 0.32 cm O.D. teflon tubes linking all these to each other was brought out of the sterile hood and arranged as shown in Figure 5.1. The liquid outlet needles were removed from the wrapping of autoclave paper and wiped with alcohol swabs before insertion into the bottles.

After assembling the apparatus, the needle and the tube belonging to the bottle containing KRBH + 20 mM glucose was filled with the buffer solution. The filling was stopped when the liquid emerged from the 3-way valve and proceeded into the tube

leading to the pump. The valve was then adjusted to allow flow of the glucose free KRBH. The pump was primed and the delivery device held inclined while it filled. The CSTR was then inclined slightly and filled so as to eliminate potential air bubbles. The stir plate under the CSTR was set at 30 rpm and the incubator door shut, to be opened only at the end of the experiment. The fraction collector containing 135 test tubes was set to collect samples every 2 min. The flowrate was adjusted to 3.0 ml/min so that each test tube would have a sample volume of 6 ml.

The experiment consisted of four phases each lasting one hour. Phase 1 (first hour) consisted of exposing the cells to glucose free KRBH in order to determine the basal concentration of insulin in the liquid. In Phase 2 (second hour), the cells were exposed to KRBH containing 20 mM glucose to determine the concentration of insulin when the cells were stimulated. During the third phase, NO was introduced into the buffer solution via the delivery device to observe the effect of NO on the cells. In the fourth and final phase, the NO was turned off to see whether the insulin concentration would readjust to pre-NO exposure levels. This was to observe whether the effect of NO was temporary or permanent.

5.4 Insulin RIA of the samples.

Thirty samples were collected for each phase of the experiment. Six evenly spaced samples from each set of 30 were selected for the insulin assay. The assay was conducted using Dr. MaCann's facilities in the School of Veterinary Medicine, Oklahoma State University. The assay used five insulin standards prepared with human insulin (RIA kit purchased from Diagnostic Products Corporation, Los Angeles, CA). The standards were

0, 5, 15, 50 and 200 μU/ml of insulin respectively. There were also two samples containing known concentrations of insulin. These were used to test the accuracy of the calibration.

5.4.1 Principle of the assay.

The assay involves the use of test tubes coated on the inside with insulin antibody. A sample containing insulin and a tracer containing radioactive I^{125} labeled human insulin are pipetted into a tube one after the other. The radioactive insulin and human insulin bind competitively with the antibody. The radioactivity in the tube is then measured using a gamma counter. The concentration of normal insulin is inversely proportional to the amount of radioactivity detected.

5.4.2 Assay procedure.

The insulin assay was conducted using the prepared standards and tracer already available in Dr. MaCann's laboratory. Each sample/standard is pipetted into two RIA test tubes and the final concentration is an average of the two values obtained from the test tubes. Since six samples were selected from each of the four phases, there were a total of 24 samples. In addition, there were five standards and two test samples. Two polyethylene test tubes containing only the tracer were also used. Initially the tubes were numbered from 1 to 64 beginning with the polyethylene tubes. Following this, 200 μl of each sample/standard was pipetted into two tubes beginning with the standard containing no insulin. A different pipette tip was uses for each sample/standard. Next, 1.0 ml of tracer was pipetted into each tube. The tubes were then arranged in a test tube rack,

covered with aluminum foil, and agitated by shaking to improve mixing of the contents. The test tubes were then incubated in a water bath at 37°C for three hours. At the end of three hours, the liquid from the tubes was decanted and the tubes shaken dry. The test tubes were then transferred to racks used with the gamma counter. The racks were placed in the gamma counter and the assay of the radioactivity begun after selecting the appropriate protocol. The gamma counter assayed the various tubes and provided a printout of the results.

5.5 Results.

The results of the assay indicated that the insulin concentrations were (0.20-0.75 μU/ml). These values are lower than the sensitivity (1.5 μU/ml) of the assay. The data points were scattered showing no obvious trend and a lot of the time, even the readings from the two tubes containing the same sample were very different. However, 2-3 samples from each phase of the experiment had similar values of insulin concentration. Assuming this to be the general trend in that phase of the experiment, the readings from tubes having values very much higher or lower than the generally similar value were discarded. The remaining values of insulin concentration (μU/ml) were plotted with time as shown in Figure 5.2. The plot displays an approximate basal insulin concentration of 0.13 μU/ml estimated from samples collected in the first hour. With glucose stimulation (second hour), a steady rise is observed in the insulin concentration. During the third hour when the cells are exposed to NO, the insulin concentration decreases from ~0.3 μU/ml to ~0.2 μU/ml. The fourth hour of exposing the cells to NO free buffer fails to bring the

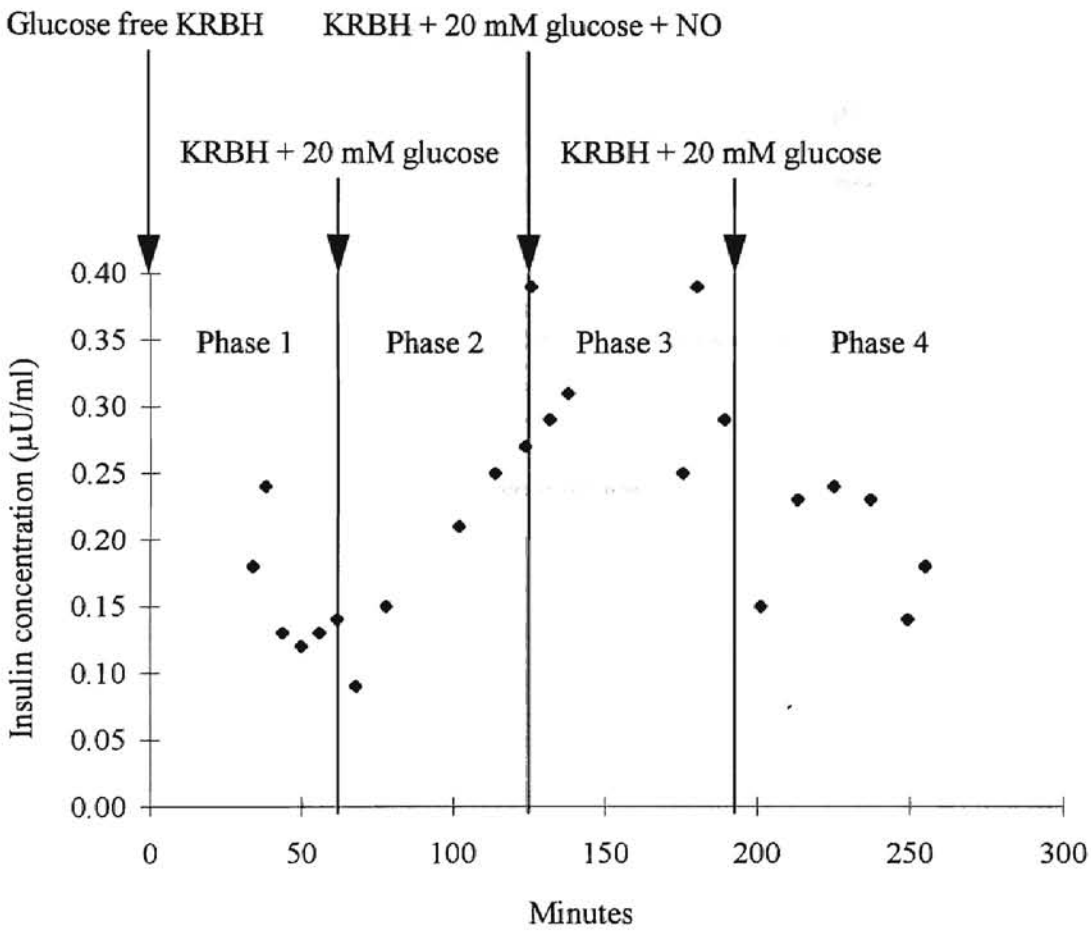

Figure 5.2. Effect of NO on insulin secretion.

insulin concentration back to the levels of Phase 2 indicating a permanent decrease in the secretion rate of insulin.

The results of a second experiment were very sporadic which prevented meaningful iterpretation. Again, the insulin concentrations measured had lower values than the sensitivity of the assay.

5.6 Problems encountered in the experiment.

There were two main problems that were noticed during the experiment. At the end of the experiment when the CSTR was inspected, a lot of air bubbles were present. The cause could either be a leak upstream or a leak in the CSTR itself. The first seems to be a more plausible reason because a leak in the CSTR has never before been noticed and the fact that the o-rings are used in the CSTR to seal the contact between the lower vessel and the plexiglas. Furthermore, no bubbles were noticed upstream of the delivery device so the leak must have been in the delivery device. Although this problem had not yet been confronted, the possibility for a leak of air into the liquid exists as it is only the membrane itself that seals the joint between the plexiglas and the central steel part. Also the stirbar had a considerable amount of rust deposited on it. Closer inspection revealed that the gold layer covering the magnetic steel had worn off at the surfaces of contact with the CSTR. Somehow, the presence of several components in the buffer, several of which are salts, had accelerated the rust formation. The remedy to this problem is to replace the stirbar with one made of teflon as explained earlier in Chapter 4, Section 4.3.3.

5.7 Problems with the assay.

Several facts came to light after the first assay. Primarily, the number of cells need to be increased to bring the insulin concentrations to values that are higher than the sensitivity of the assay. Secondly, the assay uses human insulin standards whereas the INS-1 cells synthesize rat insulin.

5.8 Conclusions.

The results clearly demonstrate that the designed apparatus is feasible for use in delivering NO to cells. In the light of the results, it seems extracellular NO inhibits insulin secretion by pancreatic β-cells. A reliable assay would lend greater credibility to the results and is essential for achieving future goals.

CHAPTER 6

CONCLUSIONS AND RECOMMENDATIONS

A novel and reliable method for NO delivery that eliminates the presence of species other than NO and nitrite in the liquid was developed. Previous cell experiments using NO-donor-compounds to deliver NO to cells had drawbacks. There was uncertainty in interpreting the results produced by the experiments due to the presence of several species in addition to NO which could have caused harm to the β-cells. In addition, the experimental apparatus used did not ensure that cells were exposed to uniform and steady-state NO concentrations. Therefore, an apparatus capable of delivering a wide range of NO concentrations in the liquid with relatively minor modifications was developed. This method of NO delivery eliminates the major shortcomings observed in previous experiments using NO-donor compounds by providing an environment in which pancreatic β-cells are exposed to uniform and steady-state NO concentrations devoid of other damaging species.

The delivery of NO in the liquid was modeled. The measured values of the NO concentrations in the CSTR fall within ±7% of the model predictions at 37°C. Thus the model has thus been successfully validated as required by Aim #2 and will prove useful in achieving future goals by accurately predicting the NO concentration to which the cells are exposed.

Finally, the apparatus was demonstrated to work reliably in experiments using cells. A detailed procedure for setup and conduct of experiments was worked out for performing experiments using β-cells. This method has the advantage that it can be used to evaluate the effects of NO on a variety of different mammalian cells without any major modifications.

6.1 Conclusions.

In the light of the preceding observations the following conclusions are reached:

- the mass transfer model accurately predicts the NO concentration at the delivery device outlet.
- the stirred vessel behaves as an ideal CSTR.
- the reaction model accurately predicts the NO concentration in the stirred vessel.
- it is feasible to use the designed apparatus in experiments with cells.
- the thesis aims have been achieved.

6.2 Recommendations.

The goals in the immediate future are to use this model and delivery method for determining the effect of extracellularly generated NO on β-cells from rats. A better assay should be developed using rat insulin to prepare the standards for calibration. A method of determining the percentage of dead cells should also be established to evaluate the effect of NO on cell viability. The next step should then be to use human β-cells. Experiments should be performed using a monolayer of β-cells as well as whole human

islets to see if NO affects the β-cell viability and function in the same way and to the same extent in either case.

Experiments could also be performed using culture medium containing one or a combination of several cytokines. The NO generation induced by the cytokines could be measured using the probe while also determining the effect of cytokines on insulin secretion and cell viability. The cytokine concentration could be varied by changing the concentrations in the culture medium. The simultaneous effect of exposing cells to extracellularly and intracellularly generated NO could be examined by concomitantly using the delivery device to deliver NO to cells.

A suggestion regarding improvements to the present design of the CSTR is to replace the stirbar currently in use with a identically sized stir bar made of teflon constructed as explained in Section 4.3.3. Another suggestion with regard to the CSTR is to cut out the bottom and replace it with an identical removable bottom occupying the same position. This removable bottom would make it easier to remove the disc containing the cells after the experiment, facilitating subsequent staining and determination of the number of dead cells. In order to eliminate potential leaks in the delivery device, the membrane should be stuck to the plexiglas as well as the central part.

REFERENCES

Anderson, H.U., Jorgensen, K.H., Egeberg, J., Mandrup-Poulson, T. and Nerup, J. (1994) Nicotinamide prevents interlukin-1 effects on accumulated insulin release and nitric oxide production in rat islets of Langerhans. *Diabetes* **43**, 770-777.

Asfari, M., Janjic, D., Meda, P., Li, G., Halban, P.A. and Wollheim, C.B. (1992) Establishment of 2-mercaptoethanol dependent insulin-secreting cell lines. *Endocrinology* **130**, 167-178.

Beckman, J.S., Beckman, T.W., Chen, J., Marshall, P.A. and Freeman, B.A. (1990) Apparent hydroxyl radical production by peroxinitrite: Implication for endothelial injury from nitric oxide and superoxide. *Proc Natl Acad Sci USA* **88**, 10860-10864.

Bendtzen K. (1989) Immune hormones (cytokines); pathogenic role in rheumatic and endocrine diseases. *Autoimmunity* **2**, 177-189.

Bonner-Weir, S. (1991) Anatomy of the islet of Langerhans. In E. Samols (Ed.). The endocrine pancreas (pp. 18-19). New York: Raven Press.

Burleigh, D.E. (1992) N^g-nitro-L-arginine reduces nonadrinergic, noncholinergic relaxations of human gut. *Gastroenterology* **102**, 679-683.

Castano, L. and Eisenbarth, G.S. (1990) Type-I diabetes: A chronic autoimmune disease of human, mouse, and rat. *Annu Rev Immunol* **8**, 647-679.

Cleeter, M.W.J., Cooper, J.M., Darley-Usmar, V.M., Moncada, S. and Scapira, A.H.V. (1994) Reversible inhibition of cytochrome oxidase, the terminal enzyme of the mitochondrial respiratory chain, by nitric oxide. *FEBS Lett* **345**, 50-54.

Collingridge, G.L., Kehl, S.J. and McLennan, H. (1983) Excitatory amino acids in synaptic transmission in the Schaffer colletral-commissural pathway of the rat hippocampus. *J Physiol (Lond)* **334**, 33-46.

Colton, C.K. and Lowrie, E.G. (1981) Hemodialysis: Physical principles and technical considerations. In B.M. Brenner and F.C. Rector, Jr. (Eds.). The Kidney (2nd Ed.) (pp. 2460-2464). Philadelphia: Saunders.

Conner, E.M. and Grisham, M.B. (1993) Nitric Oxide: Biochemistry, Physiology, and Pathophysiology. *Methods* **7**, 3-13.

Coolman, R.M. and Robarge, W.P. (1995) Sampling nitrous oxide emissions from humid tropical ecosystems. *J Biogeography* **22**, 381-391.

Corbett, J.A. and McDaniel, M.L. (1992) Does nitric oxide mediate autoimmune destruction of β-cells?: Possible therapeutic interventions in IDDM. *Diabetes* **41**, 897-903.

Corbett, J.A. and McDaniel, M.L. (1995) Intraislet release of interlukin 1 inhibits β-cell function by inducing β-cell expression of inducible nitric oxide synthase. *J Exp Med* **181**, 559-568.

Corbett, J.A., Wang, J.L., Hughes, J.H., Wolf, B.A., Sweetland, M.A., Lancaster, J.R. and McDaniel, M.L. (1992) Nitric oxide and cyclic GMP formation induced by interlukin 1β in islets of Langerhans.. *Biochem J* **287**, 229-235.

Corbett, J.A., Sweetland, M.A., Wang, J.L., Lancaster Jr., J.R., and McDaniel, M.L. (1993) Nitric oxide mediates cytokine-induced inhibition of insulin secretion by human islets of Langerhans. *Proc Natl Acad Sci USA* **90**, 1731-1735.

de Belder, A.J., Radomski, M.W., Why, H.J.F., et al. (1993) Nitric oxide synthase activities in human myocardium. *Lancet* **341**, 84-85.

Delaney, C.A. and Eizirik,D.L. (1996) Intracellular targets for nitric oxide toxicity to pancreatic β-cells. *Braz J Med Biol Res* **29**, 569-579.

Delaney, C.A., Green, M.H.L., Lowe, J.E. and Green, I.C. (1993) Endogenous nitric oxide induced by interlukin-1β in rat islets of Langerhans and HIT-T15 cells causes significant DNA damage as measured by comet assay. *FEBS Lett* **333**, 291-295.

DeMaster, E.G., Raij, L., Archer, S.J. and Weir, E.K. (1989) Hydroxylamine is a vasorelaxant and a possible intermediate in the oxidative conversion of L-arginine to nitric oxide. *Biochem Biophys Res Commun* **163**, 527-533.

Drapier, J-C. and Hibbs Jr. J.B. (1986) Murine cytotoxic activated macrophages inhibit aconitase in tumor cells: Inhibition involves the iron-sulfur prosthetic group and is reversible. *J Clin Invest* **78**, 790-797.

Dunger, A., Cunningham, J.M., Delaney, C.A., Lowe, J.E., Green, M.H.L., Bone, A.J. and Green, I.C. (1996) Tumor necrosis factor-α and interferon-γ inhibit insulin secretion and cause DNA damage in unweaned-rat islets. *Diabetes* **45**, 183-189.

Eisenbarth, G.S. (1986) Type I diabetes mellitus. A chronic autoimmune disease. *N Engl J Med* **314**, 1360-1368.

Eizirik, D.L., Delaney, C.A., Green, M.A., Cunningham, J.M., Thorpe, J.R., Pipeleers, D.G., Hellerstrom, C. and Green, I.C. (1996) Nitric oxide donors decrease the function and survival of human pancreatic islets. *Mol Cell Endocr* **118**, 71-83.

Eizirik, D.L., Pipeleers, D.G., Ling, Z., Welsh, N., Hellerstrom, C. and Andersson, A. (1994) Major species difference between humans and rodents in the susceptibility to pancreatic β-cell injury. *Proc Natl Acad Sci USA* **91**, 9253-9256.

Eizirik, D.L., Sandler, S., Welsh, N., Cetkovic-Cvrlje, M., Nieman, A., Geller, D.A., Pipeleers, D.G., Bendtzen, K. and Hellerstrom, C. (1994) Cytokines suppress human islet function irrespective of their effects on nitric oxide generation. *Am Soc Clin Invest* **93**, 1968-1974.

Eizirik, D.L., Welsh, N. and Hellerstrom, C. (1993) Predominance of stimulatory effects of interlukin-1β on isolated human pancreatic islets. *J Clin Endocr Metab* **76**, 399-403.

Fehsel, K., Jalowy, A., Qi, S., Burkart, V., Hartmann, B. and Kolb, H. (1993) Islet cell DNA is target of inflammatory attack by nitric oxide. *Diabetes* **42**, 496-500.

Foulis, A.K. (1987) The pathogenesis of beta cell destruction in Type I (insulin-dependent) diabetes mellitus. *J Pathol* **152**, 141-148.

Green, I.C., Cunningham, J.M., Delaney, C.A., Elphick, M.R., Mabley, J.G. and Green, M.G. (1993) Effects of cytokines and nitric oxide donors on insulin secretion, cyclic GMP and DNA damage: relation to nitric oxide production. *Biochem Soc Trans* **22**, 30-37.

Gustafsson, L.E., Leon, A.M., Persson, M.G., Wiklund, N.P. and Moncada, S. (1991) Endogenous nitric oxide is present in the exhaled air of rabbits, guinea pigs and humans. *Biochem Biophys Res Commun* **181**, 852-857.

Hibbs, J.B.Jr., Taintor, R.R., Vavrin, Z., et al. (1990) Synthesis of nitric oxide from a terminal guanidino nitrogen atom of L-arginine: a molecular mechanism regulating cellular proliferation that targets intracellular iron. In S. Moncada and E.A. Higgs (Eds.). Nitric oxide from L-arginine: A bioregulatory system. proceedings of the Symposium on Biological Importance of Nitric Oxide, London, September 14-15, 1989 (pp. 189-223). Amsterdam: Excerpta Medica.

Hogg, N., Darley-Usmar,V.M., Wilson, M.T., Moncada, S. (1992) Production of hydroxyl radicals from the simultaneous generation of superoxide and nitric oxide. *Biochem. J.* **281**, 419-421.

Huie, R.E. and Padmaja, S. (1993) The reaction of NO with superoxide. *Free Rad Res Comms* **18**,195-199.

Ignarro, L.J.,Bush, P.A., Buga, G.M., Wood, K.S., Fukuto, J.M. and Rajfer, J. (1990) Nitric oxide and cyclic GMP formation upon electrical field stimulation cause relaxation of corpus cavernosum smooth muscle. *Biochem Biophys Res Commun* **170**, 843-850.

Kaneto, H., Fujii, J., Seo, H.G., Suzuki, K., Matsuoka, T., Nakamura, M., Tatsumi, H., Yamasaki, Y., Kamada, T. and Taniguchi, N. (1995) Apoptotic cell death triggered by nitric oxide in pancreatic β-cells. *Diabetes* **44**, 733-738.

Kawahara, D.J. and Kenney, J.S. (1991) Species difference in human and rat islets to human cytokines. Monoclonal anti-interlukin-1 (IL-1) influences on direct and indirect IL-1 mediated islet effects. *Cytokine* **3**, 117-124.

Kerwin Jr., J.F., Lancaster Jr., J.R. and Feldman, P.L. (1995) Nitric oxide: A new paradigm for second messengers. *J Med Chem* **38**, 4343-4362.

Kolb, H. and Kolb-Bachofen, V. (1992) Nitric oxide: a pathogenic factor in autoimmunity. *Immunology Today* **13**, 157-160.

Kowaluk, E.A. and Fung, H-L. (1990) Spontaneous liberation of nitric oxide cannot account for *in Vitro* vascular relaxation by S-nitrosothiols. *J Pharmacol Exp Ther* **255**, 1256-1264.

Kroncke, K-D., Brenner, H-H., Rodriguez, M-L., Etzkorn, K., Noack, E.A., Kolb, H. and Kolb-Bachofen, V. (1993) Pancreatic islet cells are highly susceptible towards the cytotoxic effects of chemically generated nitric oxide. *Biochim Biophys Acta* **1182**, 221-229.

Kroncke, K-D., Fehsel, K. and Kolb-Bachofen, V. (1995) Inducible nitric oxide synthase and its product nitric oxide, a small molecule with complex biological Activities. *Biol. Chem. Hoppe-Seyler* **376**, 327-343.

Kubes, P., Suzuki, M. and Granger, D.N. (1991) Nitric oxide: An endogenous modulator of leukocyte adhesion. *Proc Natl Acad Sci USA* **88**, 4651-4655.

Lange, N.A. Lange's Handbook of Chemistry. rev. 10th edition (1967), McGraw Hill New York, NY, 1099-1101.

Lewis, R.S. (1995) Nitric oxide kinetics in biological systems., PhD thesis, Massachusetts Institute of Technology, Cambridge, MA (pp. 47-49, 79).

Lewis, R.S. and Deen, W.M. (1994) Kinetics of the reaction of nitric oxide with oxygen in aqueous solutions. *Chem Res Toxicol* **7**, 568-574.

Mandrup-Poulson, T., Helqvist, S., Wogensen, L.D., Molvig, J., Pociot, F., Johannesen, J. and Nerup, J. (1990) Cytokines and free radicals as effector molecules in the destruction of pancreatic beta cells. *Curr Top Microbiol Immunol* **164**, 169-193.

McDaniel, M.L., Kwon, G., Hill, J.R., Marshall, C.A. and Corbett, J.A. (1996) Cytokines and nitric oxide in islet inflammation and diabetes. *Proc Soc Exp Bio Med* **211**, 24-32.

Mearin, F., Mourelle, M., Guarner, F., et al. (1993) Patients with achalasia lack nitric oxide in gastro-oesophagial junction. *Eur J Clin Invest* **23**, 724-728.

Moncada, S. (1992) The L-arginine: nitric oxide pathway. *Acta Physiol Scand* **145**, 201-227.

Moncada, S. (1994) Nitric oxide. *J Hypertension.* **12** (suppl 10), S35-S39.

Moncada, S. and Higgs, A. (1993) The L-arginine-nitric oxide pathway. In F.H. Epstein (Ed.). *N Engl J Med* **329**, 2002-2012.

Moncada, S., Palmer, R.M.J. and Higgs, E.A. (1989) Biosynthesis of nitric oxide from L-arginine: a pathway for regulation of cell function and communication. *Biochem. Pharmacol* **38**, 1709-1715.

Nathan, S. and Sporn, M. (1991) Cytokines in context. *J Cell Bio* **113**, 981-986.

Panagiotidis, G., Akesson, B., Rydell, E.L. and Lundquist, I. (1995) Influence of nitric oxide synthase inhibition, nitric oxide and hydroperoxide on insulin release induced by various secretagogues. *Brit J Pharmacol* **114**, 289-296.

Pepko-Zaba, J., Higenbottam, T.W., Dinh-Xuan, A.T., Stone, D. and Wallwork, J. (1991) Inhaled nitric oxide as a cause of selective pulmonary vasodilation in pulmonary hypertension. *Lancet* **338**, 1173-1174.

Pukel, C., Baquerizo, H. and Rabinovitch, A. (1988) Destruction of rat islet cell monolayers by cytokines: Synergistic interactions of inerferon-g, tumor necrosis factor, lymphotoxin, and interlukin-1. *Diabetes* **37**, 133-136.

Rabinovitch, A., Suarez-Pinzon, W.L., Sorensen, O. and Bleackley, R.C. (1996) Inducible nitric oxide synthase (iNOS) in pancreatic islets of nonobese diabetic mice: Identification of iNOS-expressing cells and relationships to cytokines expressed in the islets. *Endocrinology* **137**, 2093-2099.

Rabinovitch, A., Suarez-Pinzon, W.L., Strynadka, K., Shulz, R., Lakey, J.R.T., Warnock, G.L. and Rajotte, R.V. (1994) Human pancreatic islet b-cell destruction by cytokines is independent of nitric oxide production. *J Clin Endocr Metab* **79**, 1058-1062.

Rabinovitch, A., Sumoski, R.V., Rajotte, R.V. and Warnock, G.L. (1990) Cytotoxic effects of cytokines on human pancreatic islet cells in monolayer culture. *J Clin Endocr Metab* **71**, 152-156.

Radi, R. (1996) Reactions of nitric oxide with metalloproteins. *Chem Res Toxicol* **9**, 828-835.

Radomski, M.W. and Moncada, S. (1991) Biological role of nitric oxide in platelet function. In S. Moncada, E.A. Higgs and J.R. Barrazueta. (Eds.) Clinical relevance of nitric oxide in the cardiovascular system (pp. 45-46). Madrid: EDICOMPLET.

Ramamurthi, A. (1996) Characterization and modeling of nitric oxide release in aqueous solutions., Masters Thesis, Oklahoma State University, Stillwater, OK (pp.44-45).

Rand, M.J. (1992) Nitrergic transmission: Nitric oxide as a mediator of non-adrenergic, non-cholinergic neuro effector transmission. *Clin Exp Pharmacol Physiol* **19**, 147-169.

Rossaint, R., Falke, K.J., Lopez, F., Slama, K., Pison, U. and Zapol, W.M. (1993) Inhaled nitric oxide for the adult respiratory distress syndrome. *N Engl J Med* **328**, 399-405.

Santerre, R.F., Cook, R.A., Crisel, R.M.D., Sharp, J.D., Schmidt, R.J., Williams, D.C. and Wilson, C.P. (1981) Insulin synthesis in a clonal cell line of simian virus 40-transformed hamster pancreatic beta cells. *Proc Natl Acad Sci USA* **78**, 4339-4343.

Stamler, J.S., Simon, D.I., Osborne, J.A., Mullins, M.E., Jaraki, O., Michel, T., Singel, D.J. and Loscalzo, J. (1992) S-Nitrosylation of proteins with nitric oxide: Synthesis and characterization of biologically active compounds. *Proc Natl Acad Sci USA* **89**, 444-448.

Suarez-Pinzon, W.L., Strynadka, K., Shulz, R. and Rabinovitch, A. (1994) Mechanisms of cytokine induced destruction of rat insulinoma cells: The role of nitric oxide. *Endocrinology* **134**, 1006-1010.

Tam, F.S-F. and Hiller, K. (1992) The role of nitric oxide in mediating non-adrenergic non-cholinergic relaxation in longitudinal muscle of human taenia coli. *Life Sci* **51**, 1277-1284.

Tannenbaum, S.R., Tamir, S., de Rojas-Walker, T. and Wishnok, J.S. (1991) DNA damage and cytotoxicity by nitric oxide. Proc. ACS Symposium on N-Nitroso compounds, Wash., DC.

Vallance, P. and Moncada, S.(1991) Hyperdynamic circulation in cirrhosis: a role for nitric oxide? *Lancet* **337**, 776-778.

Vanderwinden, J-M., Mailleux, P.,Schiffmann, S.N., Vanderhaeghen, J-J. and De Laet, M-H. (1992) Nitric oxide synthase activity in infantile hypertropic pyloric stenosis. *N Engl J Med* **327**, 511-515.

Volund, A. (1993) Conversion of insulin units to SI units. *Am J Clin Nutr* **58**, 714-715.

Welsh, N., Eizirik, D.L. and Sandler, S. (1994) Nitric oxide and pancreatic b-cell destruction in insulin dependent diabetes mellitus: Don't take NO for an answer. *Autoimmunity* **18**, 285-290.

Welsh, N. and Sandler, S. (1992) Interlukin-1β induces nitric oxide production and inhibits the activity of aconitase without decreasing glucose oxidation rates in isolated mouse pancreatic islets. *Biochem Biophys Res Commun* **182**, 333-340.

Zuccollo, A., Cueva, F., Frontera, M. and Catanzaro, O.L. (1995) Nitric oxide as a mediator of insulitis in type I diabetes. *Comunicaciones Biologicas* **13**, 35-42.

VITA

Shravan Nagarajan

Candidate for the degree of

Master of Science

Thesis: DESIGN AND MODEL OF NITRIC OXIDE DELIVERY TO CELLS

Major field: Chemical Engineering

Biographical:

Personal Data: Born in Madras, India, On September 2, 1971, the son of Vijaya and R. Nagarajan.

Education: Graduated from K.C.College of Science, Bombay, May 1990; received Bachelor of Engineering degree in Petrochemical Engineering from University of Poona, Pune, India, June 1994; completed the requirement for a Master of Science degree at Oklahoma State University in May, 1997.

Experience: Intern at Asian Paints (India) Ltd., Ankleshwar, India, from June 1993 to August 1993. Graduate Research Assistant, Department of Chemical Engineering, Oklahoma State University, August 1995 to December 1996 and May 1996 to December 1996. Teaching Assistant, Department of Chemical Engineering, Oklahoma State University, August 1994 to May 1995 and January 1996 to May 1996.

Memberships: AICHE (Affiliate Member).
Omega Chi Epsilon-Chapter Mu.